

KINETIC STUDIES OF THE THERMAL DECOMPOSITION OF EXPLOSIVES
USING ACCELERATING RATE CALORIMETRY

by

Pauline P. Lee

A thesis submitted in partial fulfilment
of the requirements for the degree of
Master of Science
in the
Department of Chemistry
University of Ottawa
Ottawa, Canada
1986

Margaret H. Back

Margaret H. Back

Professor of Chemistry,

Research Supervisor

Pauline Lee

Pauline Lee

M.Sc. Candidate



UMI Number: EC55786

INFORMATION TO USERS

The quality of this reproduction is dependent upon the quality of the copy submitted. Broken or indistinct print, colored or poor quality illustrations and photographs, print bleed-through, substandard margins, and improper alignment can adversely affect reproduction.

In the unlikely event that the author did not send a complete manuscript and there are missing pages, these will be noted. Also, if unauthorized copyright material had to be removed, a note will indicate the deletion.

UMI[®]

UMI Microform EC55786
Copyright 2011 by ProQuest LLC
All rights reserved. This microform edition is protected against
unauthorized copying under Title 17, United States Code.

ProQuest LLC
789 East Eisenhower Parkway
P.O. Box 1346
Ann Arbor, MI 48106-1346

ACKNOWLEDGEMENTS

I express my sincere thanks to my supervisor, Dr. Margaret Back for her guidance and encouragement throughout the performance of this work. With deep gratitude the author wishes to thank the Manager of the Canadian Explosives Research Laboratory, Mr. Ron Vandebek, for allowing me the opportunity to complete the experimental work in his laboratory.

TABLE OF CONTENTS

	page
ACKNOWLEDGEMENTS	i
LIST OF TABLES	v
LIST OF FIGURES	vi
ABSTRACT	vii
CHAPTER 1:EXPLOSIONS AND THE EVALUATION OF THERMAL STABILITY	1
I. Definition of Explosives	1
II. Classification	2
III. Uses	3
IV. Control and Assessment of Explosives	3
V. Techniques for Evaluation of Thermal Stability of Explosives	4
(a) Differential Scanning Calorimetry (DSC)	5
(b) Differential Thermal Analysis (DTA)	5
(c) Thermal Gravimetry Analysis (TGA)	6
(d) Sensitive Detector of Exothermic Process (SEDEX)	6
(e) Flowing Afterglow Spectroscopy	7
VI. The Development of the Accelerating Rate Calorimeter and the Objectives of the Present Study	8

CHAPTER 2:PRINCIPLES OF OPERATION OF THE ACCELERATING RATE	
CALORIMETER (ARC)	10
I. Thermal Explosion Theory	10
II. Theory of Adiabatic Calorimetry	11
III. Measurements using the ARC	14
CHAPTER 3:EXPERIMENTAL	17
I. Description of the Apparatus	17
(a) The Calorimeter Assembly	17
(b) Thermocouples	21
(c) Sample Bombs	22
(d) Calibration	22
II. Operation	22
III. Materials	25
CHAPTER 4:THERMAL DECOMPOSITION OF TETRYL	27
I. Properties	27
II. Previous Studies of the Decomposition of Tetryl	27
CHAPTER 5:DERIVATION OF KINETIC PARAMETERS FOR THE THERMAL	
DECOMPOSITION OF TETRYL	31
I. Experimental	31
II. Results	32
III. Calculation of the Activation Energy	38
(a) Calculation from k^*	38
(b) Calculation from Time to Maximum Rate	39
(c) Calculation from the Initial Rates	40
IV. Evaluation of Techniques	47

CHAPTER 6: ANALYSIS OF PRODUCTS	51
I. Materials and Apparatus	51
II. Procedure	52
(a) Collection of Samples	52
(b) Analysis of Products	53
CHAPTER 7: PRODUCTS, MECHANISM OF THE THERMAL DECOMPOSITION OF TETRYL	64
I. Condensed-phase Decomposition Products of Tetryl	64
II. Mechanism of the Decomposition	69
CHAPTER 8: NITROGUANIDINE	73
I. Properties	73
II. The Thermal Decomposition of Nitroguanidine	73
III. Experimental	75
IV. Results	76
A. General Features	76
B. Calculation of the Activation Energy	76
(a) Calculation from k^*	80
(b) Calculation from Time to Maximum Rate	80
(c) Calculation from the Initial Rate	80
V. Interpretation of the Activation Energy	87
CLAIMS TO ORIGINAL RESEARCH	91
REFERENCES	92

LIST OF TABLES

	page
1. Thermal decomposition data of tetryl	37
2. Calculation of the activation energy for tetryl from the relation between the self-heat rate, the temperature and the thermal inertia	46
3. Measured activation energies for the decomposition of tetryl	48
4. R _f values of tetryl, picric acid and thermal decomposition products mixture	54
5. Absorbance of solutions of tetryl and picric acid	58
6. Concentrations of equal volume mixture of tetryl and picric acid	60
7. Condensed-phase products from the decomposition of tetryl in the ARC	65
8. Thermal decomposition data of nitroguanidine	77
9. Calculation of the activation energy for nitroguanidine from the relation between the self-heat rate, the temperature and the thermal inertia	86
10. Measured activation energies for the decomposition of nitroguanidine	89

LIST OF FIGURES

	page
1. Schematic diagram of the APC showing the modifications to the assembly system	18
2. Step-heat logic of the APC	23
3. Self-heat rate, \bullet , and pressure, Δ , as a function of $1/T$ for tetryl	33
4. Rate constant, k , as a function of $1/T$ for tetryl	35
5. Time to maximum rate as a function of $1/T$ for tetryl	41
6. Self-heat rate as a function of temperature for various values of ϕ for tetryl	44
7. Absorbance as a function of wavelength, individual compound in ethanol solution	56
8. Absorbance as a function of wavelength for σ -complex of trinitroanisole in ethanol solution	61
9. Self-heat rate, A , reactant and product composition, B , as a function of $1/T$	66
10. Self-heat rate, \bullet , and pressure, Δ , as a function of $1/T$ for nitroguanidine	78
11. Time to maximum rate as a function of $1/T$ for nitroguanidine	81
12. Self-heat rate as a function of temperature for various values of ϕ for nitroguanidine	84

ABSTRACT

The thermal decomposition of the explosives, tetryl and nitroguanidine, were studied in an accelerating rate calorimeter (ARC). The influence of sample size, bomb type and pressure on the kinetics of the decomposition was investigated. Using the data obtained, three methods were applied to evaluate activation energies for the decompositions.

In the decomposition of tetryl, two maxima in the self-heat rate were observed with increasing temperature. For the decomposition in the Hastelloy C bomb, the first peak corresponded to an activation energy of $52 \pm 1 \text{ Kcal mol}^{-1}$ and the second peak indicated $43 \pm 1 \text{ Kcal mol}^{-1}$. The values obtained from the Titanium bomb were about 3 Kcal mol^{-1} lower. The wide range of values for the activation energies reported in the literature was rationalized from the point of view of the techniques used in the measurements.

The products of the thermal decomposition of tetryl, picric acid and trinitroanisole, were measured at several stages during the decomposition. At the minimum self-heat rate after the first decomposition peak, tetryl had almost completely disappeared. The trinitroanisole and picric acid accounted for 62% of the tetryl decomposed, the remainder being gaseous products and some ethanol-insoluble residue. The second peak corresponded to the decomposition of the

product picric acid. The relation of the yields of the products to the kinetics of the decomposition suggested that picric acid may not be a source of autocatalysis. The activation energy and frequency factor for the second stage of the decomposition were substantially lower than those derived from the first stage. The values obtained for the Arrhenius parameters were interpreted in terms of the type of process occurring during decomposition.

The thermal decomposition of nitroguanidine showed the characteristics of a propellant by the exceptionally fast self-heat rate. Analysis of the data of the complete decomposition gave unreasonably high values for the activation energy and frequency factor. Using data from the initial stages of the decomposition, an activation energy of $32 \pm 2 \text{ kcal mol}^{-1}$ was calculated. This behaviour was interpreted to indicate the importance of an autocatalytic process.

CHAPTER 1: EXPLOSIONS AND THE EVALUATION OF THERMAL STABILITY.

1. Definition_of_Explosives

Explosives are substances or mixtures of substances which are capable of undergoing exothermic chemical reaction at extremely fast rates, often producing high temperatures and high pressures of gaseous products. Explosives may be in the form of liquids, solids, gels or slurries. Typically they consist of a mixture of two substances, one serving as fuel and one as oxidizer. Even more rapid reaction can be produced if the oxygen and fuel are contained in a single chemical. Nitroglycerin is a compound of this type. Nitroglycerin contains sufficient oxygen to burn its carbon and hydrogen and therefore produce an extremely rapid combustion.

An explosion occurs when the confined energy is suddenly released, and may be small, as the bursting of a balloon, or large, as an atomic bomb. Between these two extremes are the commercial and military explosives where explosions are produced on a limited scale to cause specific effects. If the propagation velocity is less than the velocity of sound, 3000 m s^{-1} , the reaction wave is said to be a deflagration. If the propagation velocity of the reaction wave is supersonic, $2000\text{--}8000 \text{ m s}^{-1}$, the wave is called a detonation wave.

11. Classification

Explosives may be classified into three types:

1. Propellants (or deflagrating explosives)

These are combustible materials which burn but do not explode. Examples: black powder, smokeless powder.

2. Primary (or initiating) explosives

These explode or detonate when they are heated or subjected to spark, impact or shock. They are said to have high sensitivity. Examples: lead azide, mercury fulminate.

3. High (or secondary) explosives

High explosives detonate under the influence of the shock of the explosion of a suitable primary explosive. They differ from primary explosives in that they are not readily exploded by heat or by shock and are usually more powerful. For practical applications, all secondary explosives require the use of detonators. They are considered to have low sensitivity. Examples: dynamite, trinitrotoluene.

Explosives of all types are made for both commercial and military purposes. Many commercial explosives consist of mixtures of inorganic compounds (e.g. nitrates, metal powder) and organic compounds (e.g. aromatic nitrocompounds, nitramines, nitrate esters). Many military explosives consist of one compound or a simple mixture of explosive compounds. In such compounds, the oxygen is in the form of nitro or nitrate groups.

III. Uses

Explosives are widely used in industrial and military operations. A complete set of statistics shows a total consumption of industrial explosives in the United States in 1977 of 1,680,000 tonnes [1]. The most extensive application of explosives is in coal mining and construction. Pyrotechnic devices are now being developed for use as an inflation system for car air bags and as hot patches for repair and escape systems for aeroplanes. For military explosives, propellants are used in ammunition. High explosives are used as filling for shells, bombs and warheads of rockets.

IV. Control and Assessment of Explosives

In all countries the manufacturing, storage, transport and sale of explosives are strictly controlled by law. In Canada the licence for a factory or magazine for storage of explosives, and the importation and transportation permits are controlled by the Explosives Act and Regulations [2]. Accidental explosions may involve loss of life, injury, or damage to buildings. An understanding of the potential hazards of explosives is imperative for safe handling and operations.

Although some information concerning an explosive can be obtained by general assessment of its properties and by application of theories of explosions, its properties must

always be tested experimentally. The power of an explosive is one of the most important properties. Ballistic mortar and lead block tests are the popular tests for the strength of explosives. There are several types of sensitivity tests. The impact sensitivity is measured by the distance of travel of a falling weight into a small mass of explosive that is required to produce an explosion. Other sensitivity tests are friction test (e.g. nut and bolt), shock sensitivity (e.g. air gap) and heat test (e.g. woods metal bath). Gases and vapours produced from the firing of an explosive are also evaluated for toxicity. In each case, the test results depend on the test methods and also upon a variety of physical and chemical properties of the explosives. In terms of safety, the thermal stability of explosives plays a very important role and this is discussed in the next section.

V. Techniques for Evaluation of Thermal Stability of Explosives

All explosives are stored in magazines for a period of time after they are manufactured. Throughout this storage, it is important that the explosives remain safe and retain satisfactory properties. Thermal stability tests provide data on safety at elevated temperatures. To determine whether instability will occur, it is necessary to subject the explosive to a higher temperature than that normally encountered. Unfortunately, as the temperature increases,

the type of decomposition reaction may change. Therefore experiments at higher temperatures do not necessarily indicate the stability of the explosive under practical conditions.

For determining thermal stability, it is usual to measure the temperature at which decomposition begins. There are several techniques for such studies:

(a) Differential Scanning Calorimetry (DSC)

In this technique a fixed heating rate is applied simultaneously to a sample and a reference material contained in separate pans. The differential heat flow to the sample and reference is monitored by a thermocouple and no temperature difference is allowed. The output signal is measured in terms of heat input or heat output as a function of time or temperature. The system is used to measure the heats associated with exothermic or endothermic transitions, for example, vaporization, melting or chemical change.

(b) Differential Thermal Analysis (DTA)

In DTA, the sample and reference are heated at a controlled rate. As a sample undergoes a reaction, heat is absorbed or evolved, causing the temperature to lag behind or go ahead of the reference material. A thermogram is the plot of the difference in the temperature between sample and reference as a function of time or temperature of reference.

DTA is used primarily for studies involving high temperatures which exceed the range of DSC. Materials routinely analyzed include minerals, metal alloys, ceramics, and glasses.

(c) Thermogravimetric Analysis (TGA)

In TGA, the weight of a sample is recorded as a function of time or temperature at a controlled heating rate in a controlled atmosphere. The rate of weight change is obtained from the first derivative of the weight change with time. This technique is called derivative thermogravimetric analysis (DTG). TGA is designed for a wide variety of applications, for example, oxidative stability studies, study of decomposition kinetics, determination of the content of moisture or volatiles.

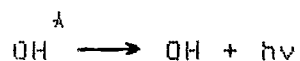
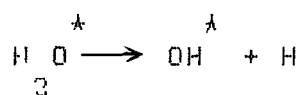
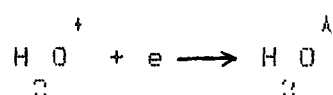
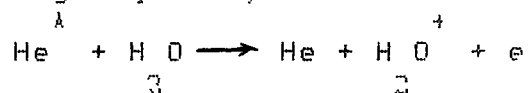
These methods have been used to determine properties of explosives such as thermal stability, kinetics of thermal decomposition and temperatures of initiation and ignition.

(d) Sensitive Detector of Exothermic Process (SEDEX)

SEDEX is an apparatus to detect the initial temperature of an exothermic process in substances under industrial operating conditions [3]. The sample is heated linearly in a receptacle by a gaseous medium. The temperatures of the heating medium and of the sample are monitored by sensors and the difference between these temperatures is recorded. This instrument has the advantages of high sensitivity, good mixing of the sample and the possibility of using a protective atmosphere.

(e) Flowing-Afterglow Spectroscopy

The flowing-afterglow method uses a small sample together with an ultra-sensitive analysis. Electronically excited rare gas atoms transfer energy to product molecules from the decomposition of the reactant, causing the formation of electronically excited fragments which undergo fluorescence. For example, with water, a common product of decomposition, excited OH radicals are formed by the following sequence,



The molecules NH_3 , CO_2 and NO_2 also form electronically excited species which readily fluoresce.

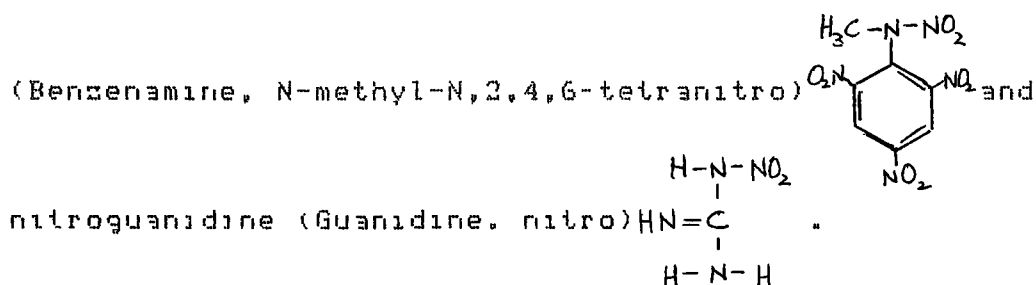
This technique was applied to the study of solid-phase thermal decomposition reactions at the Los Alamos Scientific Laboratory. It was used to study low-temperature decompositions and to measure trace amounts of certain molecules in a fast-flow system. Small amounts of moisture in helium have been detected in this manner. Emissions from a pattern of fragments often identifies a more complex molecule [4].

VI. The Development of the Accelerating Rate Calorimeter and the Objectives of the Present Study

The evaluation of thermal stability from results obtained by these techniques was not always satisfactory. Two of the main characteristics of an explosive, the temperature at which decomposition commences and the activation energy of the decomposition process, were not always obtained unambiguously. The thermal decomposition of an explosive is usually a very complex reaction, sometimes involving autocatalysis, and the mechanism of the reaction may change during decomposition. Furthermore it is difficult to compare measurements from different techniques and consequently the data cited in the literature are widely variable.

The technique of the Accelerating Rate Calorimeter was developed by Townsend and Tou at the Dow Chemical Company [5] as an alternative approach to the evaluation of thermal stability. The main difference between this technique and those described above is in the manner in which the sample is heated. Instead of applying heat, the ARC uses the heat evolved by the reactant to initiate and sustain the decomposition. Townsend and Tou discussed the kinetics of decomposition under these conditions and developed equations relating the measurements to the rate constant for decomposition.

The object of the present work was to examine the kinetics of a reaction taking place in the ARC and to evaluate the results in terms of the two characteristics mentioned earlier, the temperature at which decomposition commences and the activation energy for the decomposition process. The compounds chosen for the study were tetryl



The principles of operation of the ARC and a description of the apparatus used in this work are described in Chapters 2 and 3, respectively. Previous work on the thermal decomposition of tetryl is discussed in Chapter 4. Measurements of the rate of decomposition in the ARC and the evaluation of the activation energy for decomposition are given in Chapter 5. The analysis of the condensed-phase products is described in Chapter 6 and the correlation with the kinetics and a discussion of the mechanism is given in Chapter 7. The results of the experiments with nitroguanidine are described in Chapter 8.

CHAPTER 2: PRINCIPLES OF OPERATION OF THE ACCELERATING RATE CALORIMETER (ARC)

1. Thermal Explosion Theory

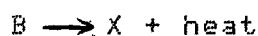
The theory of thermal explosions was quantitatively described as early as 1897 by D.L. Chapman [6]. The theory is concerned with the competition between heat generation of the reacting system and heat dissipation from the material to the surroundings. The rate of loss of heat is approximately proportional to the difference in temperature between the material and the surroundings, but the rate of generation of heat is proportional to the rate of the chemical reaction, which increases exponentially with temperature. When the rate of heat generation exceeds the rate of heat loss, a non-stationary state develops, which may lead to a runaway reaction and explosion. If the rate of heat loss equals the rate of heat generation of the reactants, the temperature will remain constant.

The original thermal explosion theory studied the conditions of stationary states and non-stationary states. Several models were developed, describing the rates of generation and loss of heat as a function of the size and the shape of the reactant and of its container and the conditions of heating [7,8]. More advanced theories described the reactant consumption, reaction mechanism and non-uniform reactant temperatures [9].

11. Theory of Adiabatic Calorimetry

In an exothermic reaction, when the heat evolution rate exceeds the heat dissipation rate, the temperature will increase and accelerate the reaction. The heat generation is a result of the chemical reaction and its rate is therefore proportional to the rate of the reaction.

For a reaction



$$-\frac{dB}{dt} = k [B] \quad (1)$$

$$k = Ae^{-E/RT} \quad (2)$$

where k is the rate constant at temperature T , A is the frequency factor, E is the activation energy and R is the gas constant. When the reactant B is not appreciably consumed, the rate of heat generation will increase exponentially with temperature.

The reaction is thus self-accelerating and the rate will increase until depletion of the reactant finally reduces the heat evolved. The rate of the reaction will pass through a maximum and finally diminish to zero at the completion of reaction at T_f . The amount of material present at any time is therefore proportional to the fractional attainment of the final temperature rise and may be expressed as

$$C = \frac{T_f - T}{T_f - T_o} C_o$$

$$\text{or } C = \frac{T_f - T}{\Delta T_s} C_o \quad (3)$$

where C_o is the initial concentration, C is the concentration at temperature T , T_o and T_f are the initial and final temperatures respectively, ΔT_s is the adiabatic temperature rise of the system.

Differentiation of equation (3) with respect to temperature gives the following expression

$$\frac{dC}{dT} = - \frac{C_o}{\Delta T_s} \quad (4)$$

For an nth order reaction, the reaction rate is

$$\frac{dC}{dt} = - kC^n \quad (5)$$

Combining equations (4) and (5) gives the rate of change of temperature in the system, called the self-heat rate, m_T which may be expressed as follows:

$$m_T = \frac{dT}{dt} = k \left(\frac{T_f - T}{\Delta T_s} \right)^n \Delta T_s C_o^{n-1} \quad (6)$$

Defining $k^* = k C_o^{n-1}$

gives
$$k^* = \frac{m_T}{\left(\frac{T_f - T}{\Delta T_s} \right)^n \Delta T_s} \quad (7)$$

For a first-order reaction, k^* is equal to k . The order of a reaction involving the decomposition of a solid material is not well defined because the concentration of a solid material is not a defined property and the characteristic of the solid which is proportional to its rate of decomposition may alter as the reaction proceeds. Therefore a rate constant for decomposition of a solid may involve some uncertainties. In many cases the rate of decomposition is approximately proportional to the amount of material and n may be taken as one. Equation (7) then becomes

$$k^* = \frac{m_T}{T_f - T} \quad (8)$$

This limitation in the definition of a rate constant for the decomposition of a solid will be discussed later in the evaluation of the Arrhenius parameters reported for decomposition of the compounds studied in this work.

III. Measurements Using the ARC

The Accelerating Rate Calorimeter measures the self-heat rate of decomposition of a substance as it undergoes self-acceleration, passes through a maximum and falls to zero. These measurements are important in the evaluation of hazard, as they provide early detection of a temperature rise or an increase in pressure. In addition, a large sample size can be used which reduces the possibility of using a non-representative sample. The results also provide information on the kinetics of the decomposition, for example, the evaluation of k^* , which may aid in understanding the mechanism of the decomposition.

In the accelerating rate calorimeter, part of the heat generated from the reaction is used to heat the sample bomb. In the experiment, the measured temperature of the sample/bomb system is dependent on the mass and the heat capacity of the bomb, the sample contact area in the bomb and the heat transfer coefficient of the material. The property of the system called the thermal inertia is defined as follows:

$$\phi = 1 + \frac{M_b C_{vb}}{M_s C_{vs}} \quad (9)$$

where M_b and M_s are the mass of bomb and sample respectively. C_{vb} is the heat capacity of the bomb and C_{vs} is the heat capacity of the sample.

The effect of thermal inertia is to slow down the reaction by a constant amount. The adiabatic temperature rise of the reactant is given by

$$\Delta T = \frac{\Delta T_{ad}}{\phi} \quad (10)$$

where ΔT is the adiabatic temperature rise and ΔT_{ad} is the temperature rise of the system. In experiments with the ARC, the thermal inertia is a critical factor in determining the rate of reaction. For perfect adiabaticity, it should be kept low, but a large thermal inertia may be useful in preventing an explosion and keeping the rate in a measurable range. The thermal inertia may be adjusted by varying the ratio of weight of sample to the weight of the bomb, or by diluting the sample with inert material. In an ideal case, ϕ is equal to one, but must be chosen to allow minimal damage to the instrument.

The heat generated per gram from the decomposition of the material in the bomb, ΔH , is given by the following equation

$$\Delta H \text{ (cal g}^{-1}\text{)} = C \frac{\Delta T_{ad}}{\phi} \quad (11)$$

and the molar heat of reaction is therefore

$$\Delta H_m \text{ (cal mol}^{-1}\text{)} = \Delta H \times \text{molecule weight} \quad (12)$$

The accelerating rate calorimeter is an automated laboratory instrument which can determine the time, temperature and pressure relationship of an exothermic reaction in an adiabatic environment. During a reaction the data is stored in a microprocessor and values of m and k^* are subsequently calculated and presented graphically.

CHAPTER 3: EXPERIMENTAL

I. Description of the Apparatus

(a) The Calorimeter Assembly

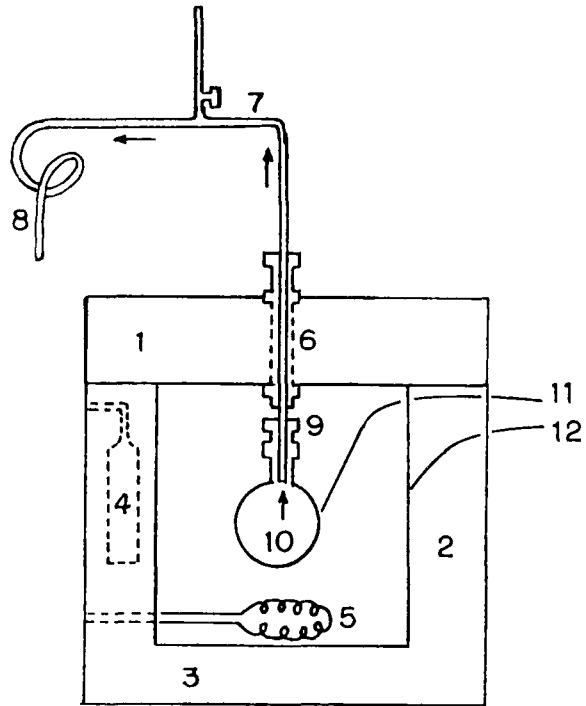
The instrument used in the present experiments was developed at Dow Chemical Company and manufactured by Columbia Scientific Industries of Austin, Texas. The Canadian Explosives Research Laboratory has used this equipment for thermal hazard evaluation of explosives and investigation of incidents since 1981 [10,11].

A diagram of the calorimeter assembly and the sample bomb used in the present experiments is shown in Figure 1. A description can be found in the literature [5, 12-15]. The bomb and its contents must be maintained adiabatically with respect to the environment so that the heat generated in the reaction is available for self-heating of the reactant. To achieve adiabatic conditions over the temperature range of ambient to 500 °C, a digital thermocouple/heater feed-back system is used to control the temperature. The calorimeter is made of copper which has high thermal conductivity and will dissipate heat input quickly. About 3 mil of nickel-plating protects the copper from high temperature oxidation. The heating jacket has three zones: top, side and bottom. The temperature of each zone is controlled independently. Eight electrical cartridge heaters are placed in the jacket for uniform heating. The thermocouples are cemented to the

Figure 1

Schematic diagram of the ARC showing the modifications
to the assembly system

1. top zone
2. side zone
3. bottom zone
4. cartridge heater
5. radiant heater
6. original fixed bomb adaptor
7. three way valve
8. 1/16 inch O.D. ss tubing connected to pressure
transducer
9. cap, connecting the 3/16 inch O.D. filler tube of
the bomb
10. sample container (bomb) with 3/16 inch O.D. filler
tube
11. bomb thermocouple
12. jacket thermocouple



inside surface of the jacket to monitor the temperature in each of the jacket zones. For self-heat measurements, one of the thermocouples, insulated with fiber-glass sleeves, is clamped directly on the outside surface of the bomb. All the thermocouples are referenced to an ice point, made by Kaye Instruments, which is stable to within 0.01 °C. The jacket is insulated with high temperature insulation to minimize heat loss to the surroundings.

Pressure is monitored with a diaphragm-type pressure transducer from Sensotec Inc., range 0-2500 psia. The transducer is mounted inside the containment vessel where it is relatively cool. For safety precautions, the entire calorimeter is placed inside a metal compartment.

When the material melts before decomposition starts, some difficulties arise. The molten material may be carried to the connecting line where it solidifies and causes a blockage. To overcome this problem, the original fixed adaptor, connecting the bomb with the pressure gauge, was replaced with a removable 1/16 inch O.D. stainless steel tubing. One end of the tubing was connected to the pressure transducer and the other end was used for connecting the sample bomb. A three way valve was installed to the line to facilitate checks for good sealing of the system and to allow release of accumulated gaseous products after the experiment. This modification reduced damage to the original fixed adaptor, provided better sealing at the connections, and

minimized blockage of the pressure measurement lines.

All the experiments were conducted in the spherical bomb under an atmosphere of air. In the "confined" system, the sample and the bomb were connected to the pressure transducer. The pressure change during the course of reaction was monitored and the products of decomposition remained in the system. Some studies were performed in a "non-confined" system in which the bomb was loosely connected to the line. The pressure in the system did not increase and the products were not confined to the bomb.

(b) Thermocouples

The successful operation of the ARC depends on sensitive, stable and reliable measurement of temperature. There should be little effects caused by annealing and oxidation. The microvolt output should not shift with time at a given temperature. Type N thermocouple (NiSi1/NiCrSi1) meets all these requirements. The selected silicon content of the alloy prevents oxidation of the metal and keeps the thermocouple output stable. Mismatch of the thermocouples may still be a problem. For example, two thermocouples which match perfectly at 25 °C may have a difference of up to 15 μ v at 300 °C. Tou [12] reported that the thermocouple attached to the side of the bomb is reliable for self-heat rates up to 70 °C/min for Ti bomb (\sim 9 g) and 30 °C/min for Hastello, (Bomb (\sim 19 g)).

(c) Sample Bombs

Spherical bombs, 1 inch O.D. diameter and 9 ml volume, were used in this study. Different materials and wall thickness gave a range of thermal inertia. The Titanium bomb had low mass and low thermal inertia. The Hastelloy C bomb had greater weight but was more corrosion-resistant. A wide-mouth cylindrical bomb made of Hastelloy C was used for testing viscous and corrosive materials.

(d) Calibration

To achieve adiabatic conditions, the jacket was maintained at the same temperature as the bomb. If drift occurred, an offset value was incorporated into the measured difference to adjust it to the correct value. The calibration was performed incrementally every 50 °C, for the entire temperature range, by applying the required voltage. The empty bomb can therefore be heated to any temperature with zero drift. During a test, a rise in temperature is therefore due to reaction.

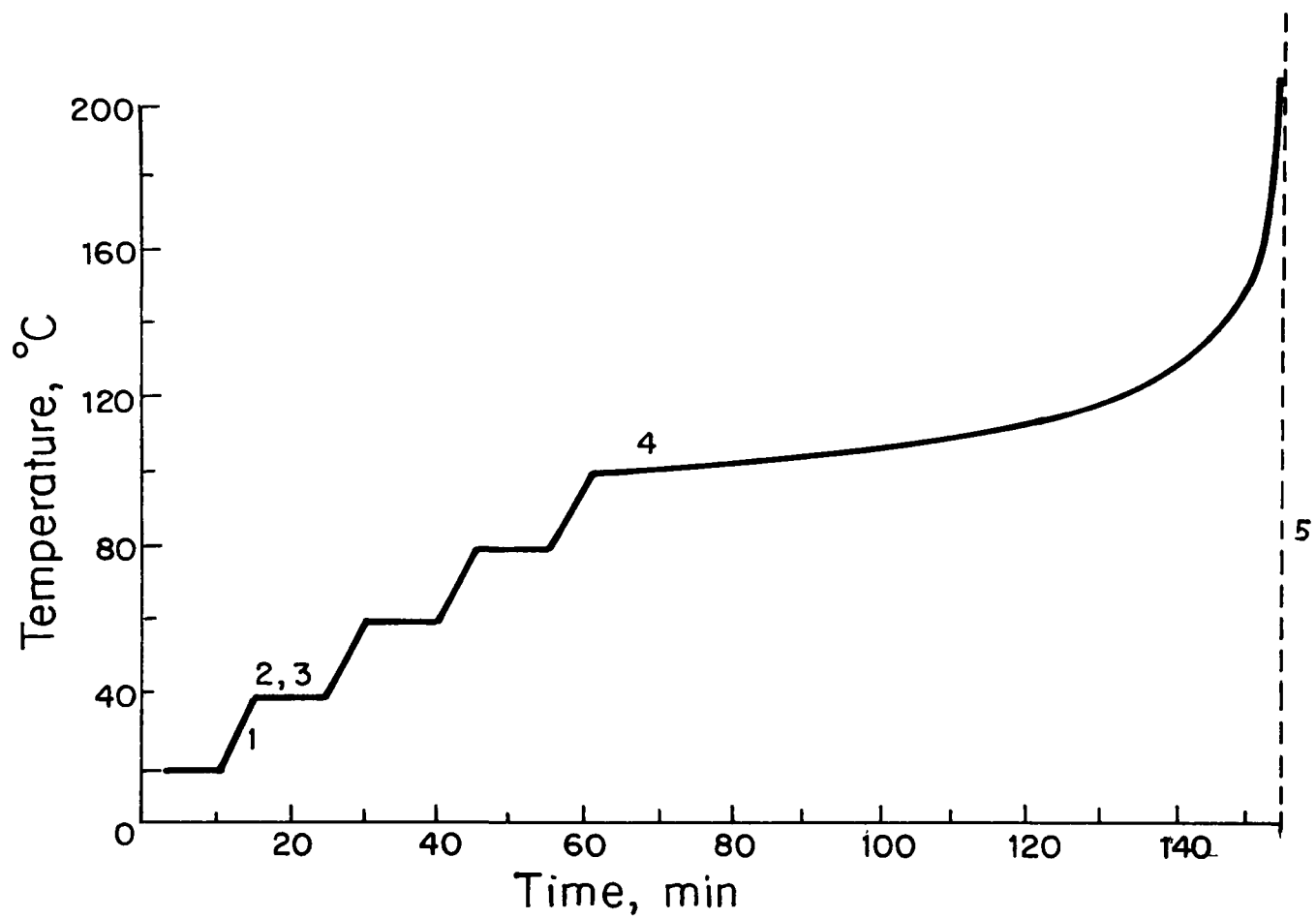
1.1. Operation

The tests were performed by the "heat-wait-search" operation logic, shown in Figure 2. The sample was first heated to the start temperature and held 30 minutes for thermal equilibrium before the rate-search operation. If a self-heat rate greater than the threshold sensitivity, 0.02
 $^{\circ}\text{C min}^{-1}$, is not detected, the ARC will proceed automatically

Figure 2

Step-heat logic of the ARC

1. heat step
2. wait step
3. search for exotherm
4. follow run away reaction
5. time of explosion



to the next "heat-wait-search" sequence. When a self-heat rate greater than the preset rate is detected, the self-accelerating reaction will be followed with data collection of time, temperature and pressure. During the reaction, the calorimeter is maintained at adiabatic condition until the completion of the reaction. At the conclusion of an experiment, the data are plotted by the microprocessor.

The isothermal age method may also be employed to study the thermal hazard of materials. Basically, the sample is maintained adiabatically at a given temperature for a long period of time, for example, several days. If a self-heat rate greater than $0.02 \text{ }^\circ\text{C min}^{-1}$ is detected during aging, the system automatically goes into the data acquisition mode until the reaction is complete. If the sample survives the aging time without reacting, then the sample is step heated to generate the self-heat curve. This method is useful for studying the effect of a catalyst or an inhibitor on the reactions.

III. Materials

The materials were stored at room temperature with no further purification before the tests. The following samples were used:

1. Military grade tetryl was obtained from Defence Research Establishment at Valcartier, Que., in the form of yellow prills.

3. Nitroguanidine with minimum purity 99% and average particle diameter 6.0-4.3 microns, was from Nigu Chemie Waldkraiburg W. Germany.

3. Silica, 240 mesh, used as diluent in the experiments, was obtained from Fisher Scientific Co.

CHAPTER 4: THERMAL DECOMPOSITION OF TETRYL

I. Properties

Tetryl (Benzenamine, N-methyl-N,2,4,6-tetranitro) is a pale yellow crystal. Pure tetryl melts at 129.5 °C and the technical products melt at 128.5-128.8 °C [16]. Tetryl is insoluble in water but is readily soluble in acetone.

The explosive properties of tetryl were examined by several authors. It is a more powerful explosive than TNT and its sensitivity to impact and friction is also higher. Because it is sensitive to initiation by a primer, it is used in detonating caps and boosters.

II. Previous Studies of the Decomposition of Tetryl

Thermal decomposition of tetryl has been studied since the early twenties [17-38]. It is generally agreed that the reaction is complex and is probably autocatalytic, but the source of the autocatalysis is not firmly established.

In an early study of the isothermal decomposition at 120 °C, Farmer [18] identified picric acid, CO, CO₂ and N₂ as the products. He suggested that picric acid caused an autocatalytic reaction. He also observed an abrupt change in rate at the melting point and found that the molten tetryl decomposed about fifty times as rapidly as the solid. Bawn [29] discussed the activation energies calculated by two investigators. When the data of decomposition of the solid

and liquid tetryl were used, an activation energy of 60 Kcal mol⁻¹ and a frequency factor of 10²⁷ s⁻¹ were calculated by Roginski. These high values were subsequently shown to be erroneous and from a re-analysis of Farmer's data, Wiseman concluded that the activation energy for decomposition of solid tetryl was 37 Kcal mol⁻¹ with a frequency factor of 10^{12.7} s⁻¹. Similar values were obtained by Robertson [20], by Cook and Abegg [21] and more recently by Hutchinson [17].

Detailed studies of the isothermal reaction were reported by Dubovitskii and co-workers [22,23]. Both condensed-phase and gaseous products were analyzed during the complete course of the decomposition. The gaseous products from the isothermal decomposition were NO, NO₂, N₂, CO and CO₂. They also analyzed the condensed-phase products at various degrees of conversion of the original substance. The products were identified as 2,4,6-trinitroanisole, picric acid and N-methyl-2,4,6-trinitroaniline by column chromatography and ultraviolet spectroscopic techniques. The presence of these compounds was interpreted to indicate that the decomposition proceeds via three parallel routes.

Several studies of the decomposition were made using thermal analytical techniques. From a DTA study, Krien [24] obtained an activation energy of 76 Kcal mol⁻¹. Rogers [25] developed a method for estimating the activation energy of a decomposition reaction by DSC, using an extremely small unweighed sample. His measurements gave an energy of

activation for the decomposition of 55 kcal mol^{-1} . A similar value was reported by Hall [26].

The more recent studies of the decomposition by DTA, TG and isothermally, are those of Hara and co-workers [27]. In the DTA study, the first exothermic decomposition occurred at 160°C and the second at 230°C . For the isothermal decomposition at $150\text{--}175^\circ\text{C}$, the rates of evolution of NO , NO_2 , N_2 and CH_4 were measured and the activation energy of the reaction was 35 kcal mol^{-1} .

Further work by Hara and Usada [28] using DTA and isothermal techniques, confirmed the simultaneous and independent formation of trinitroanisole and picric acid in the initial stages and the subsequent conversion of trinitroanisole into picric acid, first reported by Dubovitskii and co-workers [23]. They suggested that radicals formed in the initial stages, rather than picric acid, could promote the decomposition and cause an autocatalytic effect. They identified three peaks by DTA. The activation energies derived by both techniques appeared to be 41 kcal mol^{-1} .

It is clear that the understanding of the thermal decomposition of tetryl is far from satisfactory. Although the main products of the reaction, both gaseous and condensed, have been identified, their identification as primary or secondary and the activation energies for their rates of formation are not established. The purpose of the present study was to gain further understanding of the

mechanism of the decomposition by application of the new technique of accelerating rate calorimetry. Measurements by the ARC provide kinetic data for the over-all decomposition from which Arrhenius parameters may be obtained (Chapter 5). To differentiate primary and secondary products, measurements of the condensed-phase products were made in correlation with the kinetic data (Chapter 6).

CHAPTER 5: DERIVATION OF KINETIC PARAMETERS FOR THE THERMAL
DECOMPOSITION OF TETRYL.

1. Experimental

The thermal decomposition of tetryl was studied using two types of spherical bombs:

1. Titanium bomb, approximately 8 grams, filler tube size 3/16 inch O.D., 1 inch length.

2. Hastelloy C bomb, approximately 19 grams, filler tube size 3/16 inch O.D., 1/2 inch length.

Experiments were performed with values of the thermal inertia ranging from 7.4 to 21.8, obtained by using different weights of sample. For example, with 1 gram of tetryl and the bomb weighing 10 grams, and using values for C_{vb} and C_{vs} of $0.1 \text{ cal g}^{-1} \text{ } ^\circ\text{C}^{-1}$ and $0.5 \text{ cal g}^{-1} \text{ } ^\circ\text{C}^{-1}$ respectively, a value of 3 was calculated for thermal inertia from equation 9, p.14. The onset temperature of decomposition was slightly higher for the sample with greater thermal inertia. With the Hastelloy C bomb, explosion occurred when the value of θ was less than 8, causing some damage to the instrument. In one experiment, 0.3813 g of tetryl was mixed with 0.4560 g of silica, giving a value for θ of 10.3, based on the weight of tetryl. The temperature of the onset of decomposition agreed with that of the undiluted reactant. In both confined and non-confined systems, the temperature at which decomposition commenced was similar. The experiments indicated that the

Thermal decomposition of tetryl is not greatly affected by pressure or by accumulated products at an early stage. In all cases the temperature at which decomposition commenced was above the melting point of tetryl.

II. Results

Typical results of the self-heat rate and the pressure as a function of $1/T$ for the thermal decomposition of tetryl are shown in Figure 3. It is clear that the decomposition takes place in two stages. Values of k^A were obtained as a function of T , by equation 7, p.13. The linearity of the plot, $\log k^A$ as a function of $1/T$, was tested using values of the reaction order, $n=0.5, 1.0,$ and 1.5 for the two decomposition stages, and is shown in Figure 4. In the interpretation of this plot, the value of n which gives a linear relation over the widest temperature range is the most reliable indication of the order of the reaction. Both stages of the decomposition of tetryl appear to occur by a first order process. The results of the experiments are summarized in Table I. In this Table m_0 and m_m refer to the initial self-heat rate and the maximum self-heat rate, respectively. T_0 and T_m refer to the temperature at the onset of decomposition and the temperature at the maximum rate.

Figure 3
Self-heat rate, ●, and pressure, Δ, as a function of $1/T$
for tetryl. Hastelloy C bomb; $\phi = 14.2$

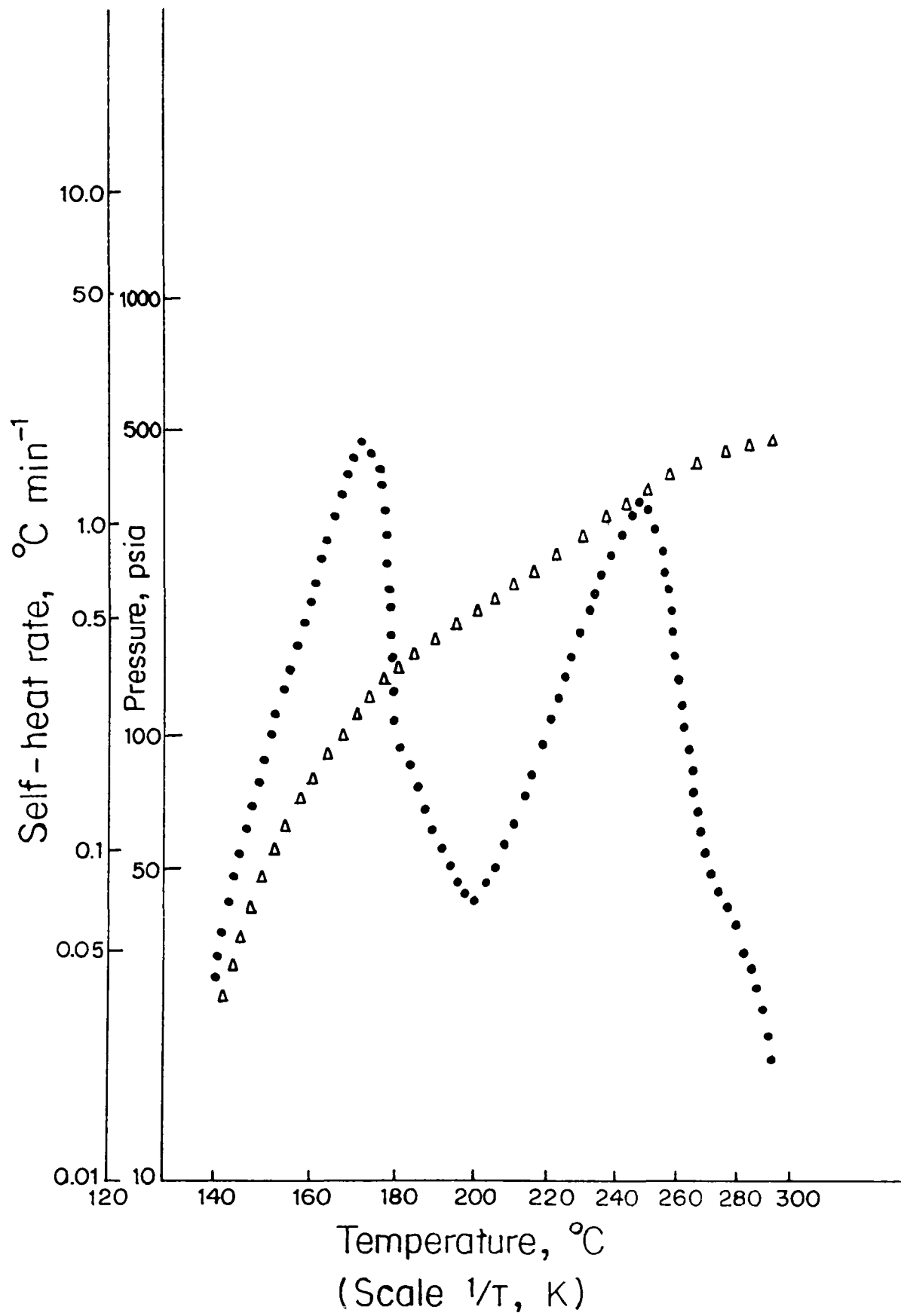


Figure 4
Rate constant, k , as a function of $1/T$ for tetryl.
Titanium bomb; $\theta = 13.4$
Reaction order, n
○ 0.5
● 1.0
△ 1.5

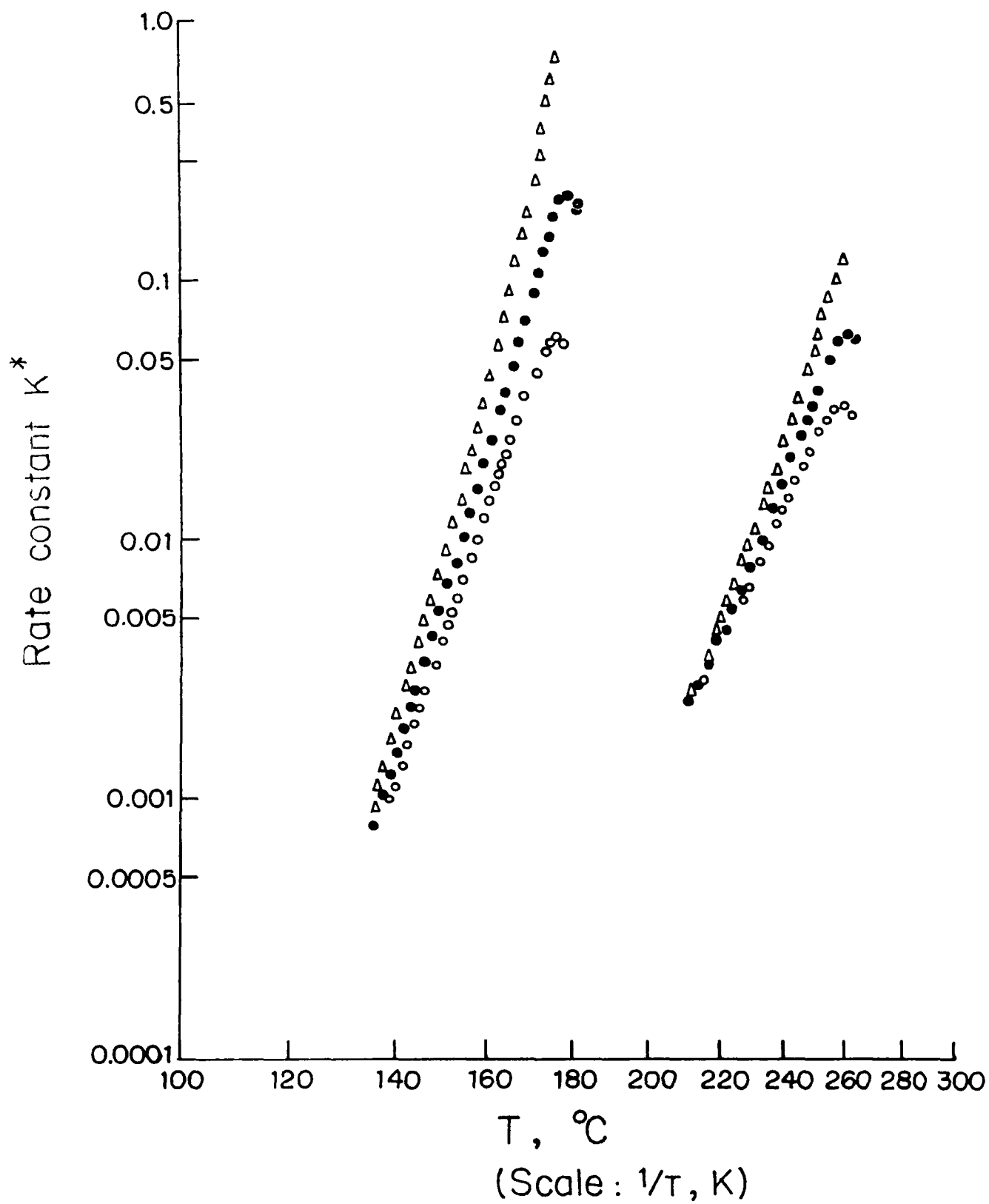


Table 1

Thermal decomposition data of tetryl

Expt #	Weight of tetryl gram	ϕ	Peak 1				Activation Energy, Kcal mol ⁻¹					
			T _o °C	m _o °C min ⁻¹	T _m °C	m _m °C min ⁻¹	Method(a)		Method(b)		Method(c)	
							Peak 1	Peak2	Peak1	Peak2	Peak 1	
Hastelloy C Bomb												
155 ^a	0.7300	7.4	136.2	0.03	183.3	161	60		53			
156	0.4256	11.8	141.5	0.04	175.1	2.50	54	46	51	48		
252	0.2546	18.7	141.0	0.03	159.6	0.26	52	42	54	40		
291	0.3552	14.2	141.5	0.04	171.5	1.24			49	42		
294	0.3550	14.2	141.7	0.05	172.8	1.76	51	43	48	38		
164 ^b	0.3813	13.0	141.4	0.04	168.5	0.78			52	37		
	Average Values							52±1	43±1	51±2	41±3	52±4
Titanium Bomb												
274	0.3868	9.1	135.9	0.03	186.5	95.5	51		48			
275	0.2510	13.5	135.9	0.02	170.1	0.88	46	38	43	36		
276	0.1500	21.8	141.1	0.04	162.2	0.24	48	41	46			
277	0.2520	13.4	136.7	0.04	174.7	1.38	50	39	45	36		
287	0.3000	11.5	140.8	0.03	176.9	1.95	50	40	45	42		
288	0.3000	11.4	140.7	0.03	171.9	1.15	50	43	49	43		
280 ^c	0.3813	10.3	140.9	0.03	181.0	4.00	46	44	44			
	Average Values							49±2	41±2	46±2	39±3	45±2

a - not included in the calculation of the average values

b - non-confined system

c - mixture of 45% Tetryl and 55% silica

1.1. Calculation of the Activation Energy

The activation energy for decomposition is one of the important parameters relating to the stability of an explosive. An activation energy is associated with a particular mechanism or pathway for decomposition and may be determined directly from a measured rate of decomposition. As discussed earlier, the rate measurement is very sensitive to the conditions of the experiment. The calculation of the activation energy from the data and its interpretation must be carefully treated. Three methods for obtaining the activation energy will be described, following the equations derived by Townsend and Tou [5]. A comparison of the values obtained by these treatments illustrates the applicability of each method in the interpretation of the mechanism of the decomposition.

1.1.1) Calculation from k^A

As discussed in chapter 2, Arrhenius parameters may be estimated directly by equation 7, p.13. This is the most direct method for obtaining the activation energy and is illustrated by the present results in Figure 4. The rate constant will be a linear function of the reciprocal of the absolute temperature provided the correct reaction order was chosen. When $\log k^A$ is a linear function of $1/T$, the slope is directly related to the activation energy (equation 2, p.11). Activation energies were calculated both from the measured slope and from the printed data points. Results

obtained for both decomposition stages are given in Table 1. The activation energy for the first stage of decomposition appeared more reproducible than that obtained for the second stage and was not greatly changed by the use of different thermal inertias. The values are, however, lower from the decomposition in the T1 bomb. The activation energy obtained from the experiment with diluent was similar to that obtained from the pure compound.

A critical factor in the calculation of k^+ is the value of T_f , the final temperature after complete decomposition. Because two stages of decomposition were obtained, a question arises concerning the separation of the two decomposition peaks and the reliability of the measured value for T_f . In the calculation of k^+ , T_f was taken at the minimum in the self-heat rate. To test the sensitivity of the values of k^+ and the activation energy to an error in T_f , k^+ was calculated using $T_f \pm 5^\circ\text{C}$. The error introduced into the activation energy ranged from 1-4%. Small uncertainties in T_f therefore have only a small effect on the activation energy. Results of the analysis of the products, described later, substantiate the validity of these values for T_f .

(b) Calculation from Time to Maximum Rate

Townsend and Tou [5] discussed the relationship between the time to maximum rate, absolute temperature, and activation energy. For a reaction with a high activation energy, the time to maximum rate, θ_m , was approximately

proportional to $1/k$, the rate constant for decomposition.

Therefore it could be expressed in the Arrhenius form

$$\ln \theta_m = \frac{E}{R} \left(\frac{1}{T} \right) - \ln A \quad (13)$$

The time to maximum rate was plotted against reciprocal of absolute temperature and a typical plot is shown in Figure 5. The linear relationship and slope of the line were determined by linear regression. The values of the activation energy for both stages obtained by this method are included in Table 1, and are in good agreement with those obtained from the first method. Again, the activation energy determined from the experiments in the Ti bomb was slightly lower than from the Hastelloy C bomb.

(c) Calculation from the Initial Rates

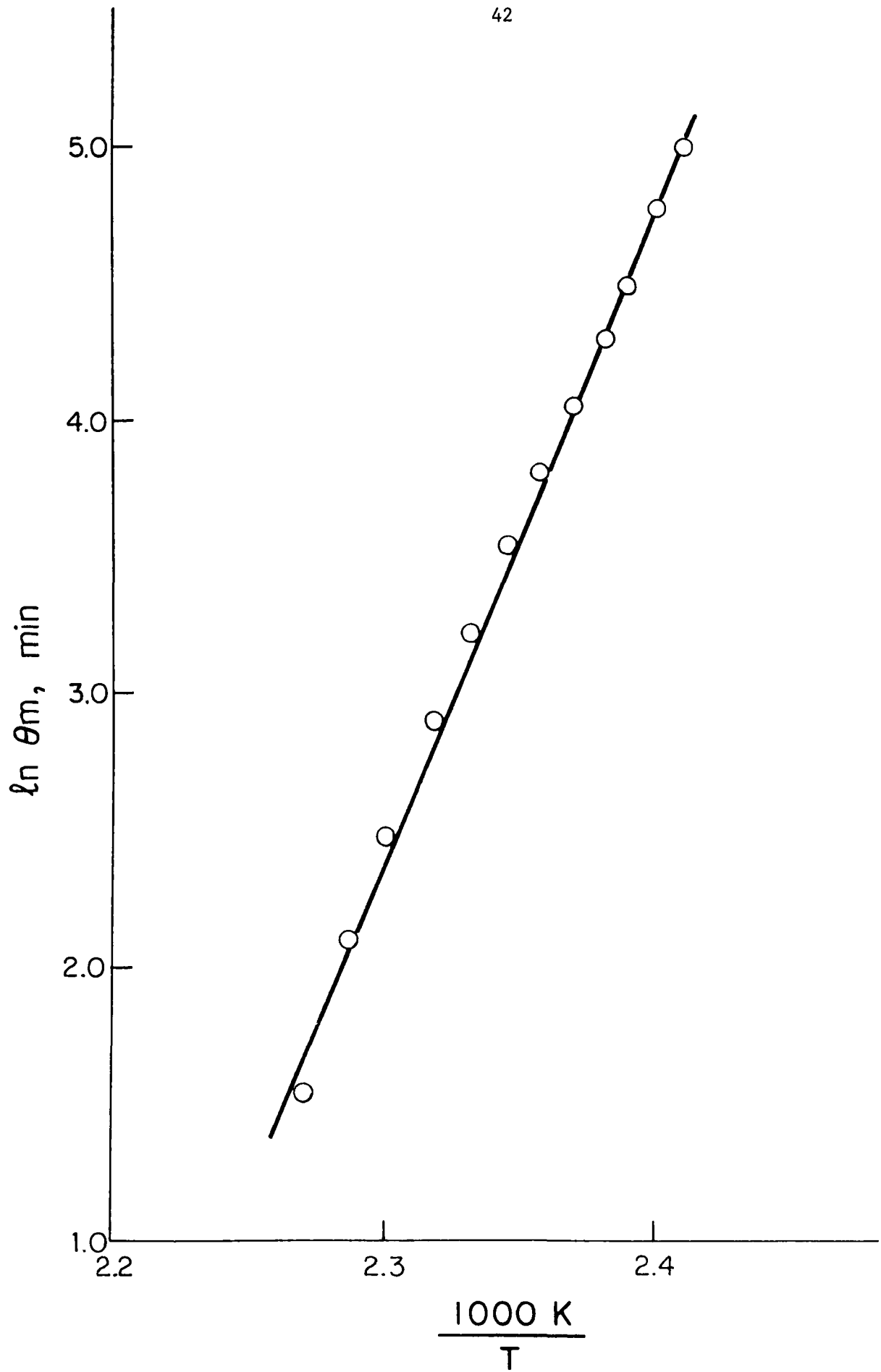
The previous methods for determination of the activation energy depend on data obtained during the complete course of the reaction. The limitation of these methods is the occurrence of a very fast self-heat rate, possibly leading to ignition, or a change in mechanism as the decomposition proceeds.

A third method uses data only in the initial stages of the reaction and therefore provides a useful comparison with the other two. As discussed previously, the onset temperature for a reaction is a function of the thermal

Figure 5

Time to maximum rate as a function of $1/T$ for tetryl.

Peak 1; Hastelloy C bomb; $\theta = 14.2$



inertia. The effect of θ is to slow down the reaction by a constant amount and this effect is a function of the activation energy of the decomposition. Townsend and Tou [5] derived a relationship involving the temperature, thermal inertia, and the activation energy for a particular self-heat rate. The equation is shown as follows:

$$\frac{1}{T_2} = \frac{1}{T_1} + \frac{R}{E} \ln \frac{\theta_1}{\theta_2} \quad (14)$$

where for experiments with thermal inertia θ_1 and θ_2 , temperatures T_1 and T_2 are obtained at a particular self-heat rate, respectively.

Because the difference in temperature for various θ is small, the self-heat rates must be accurately and reproducibly measured. If a slight drift occurs, it will cause some error in the estimation of T_1 and T_2 . The self-heat rates for different values of θ are shown as a function of temperature in Figure 6A for the T1 bomb and in Figure 6B for the Hastelloy C bomb. From the curves, T_1 and T_2 were estimated for self-heat rates of 0.05, 0.07, 0.09 and 0.10 °C min⁻¹ and the calculated activation energies are given in Table 2. The values appeared to decrease as the self-heat rate increased. This method is less accurate than the previous two because it is difficult to estimate the small temperature difference, as illustrated in Figure 6.

Figure 6

Self-heat rate as a function of temperature for
various values of ϕ for tetryl.

A: Titanium bomb

B: Hastelloy C bomb

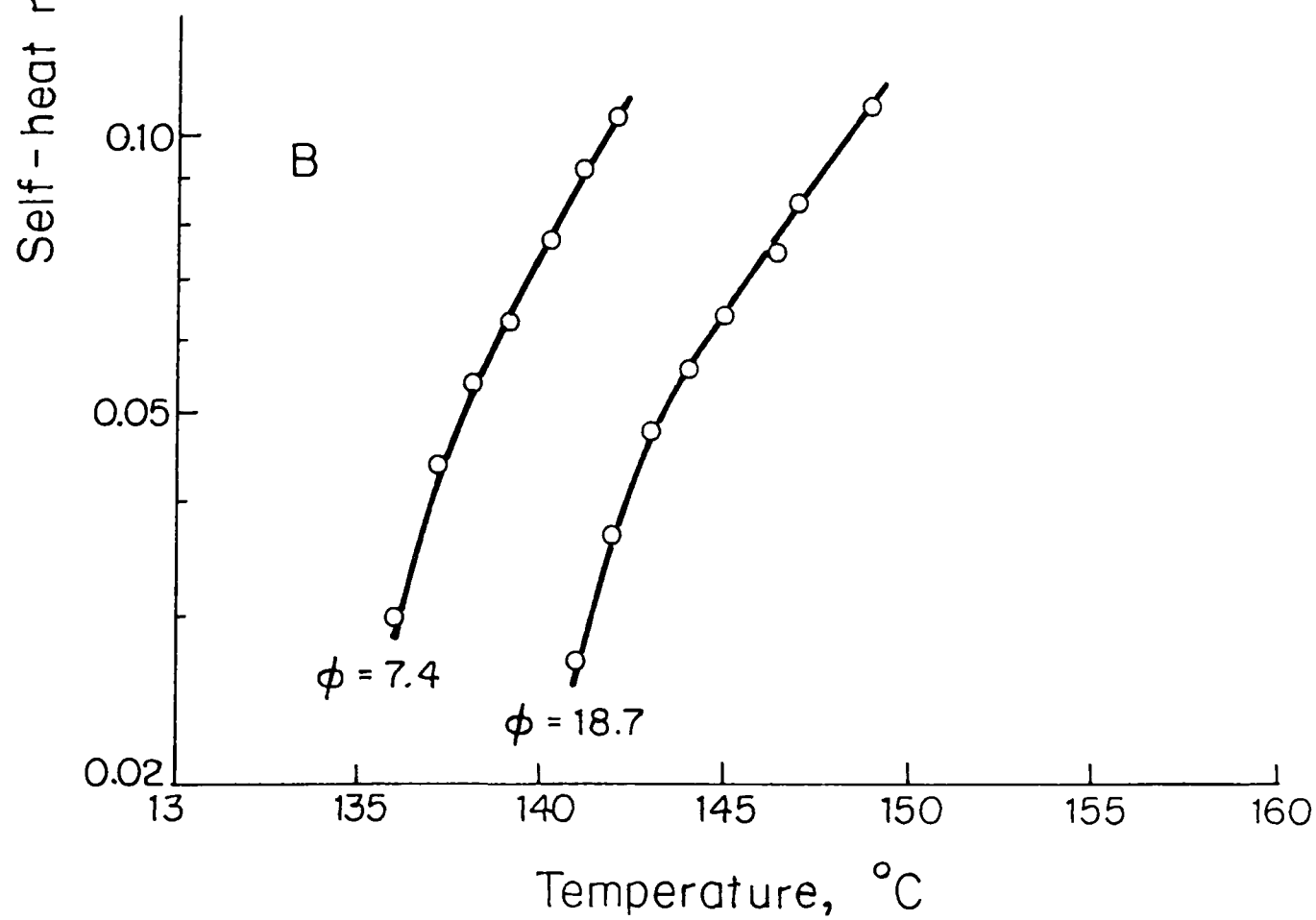
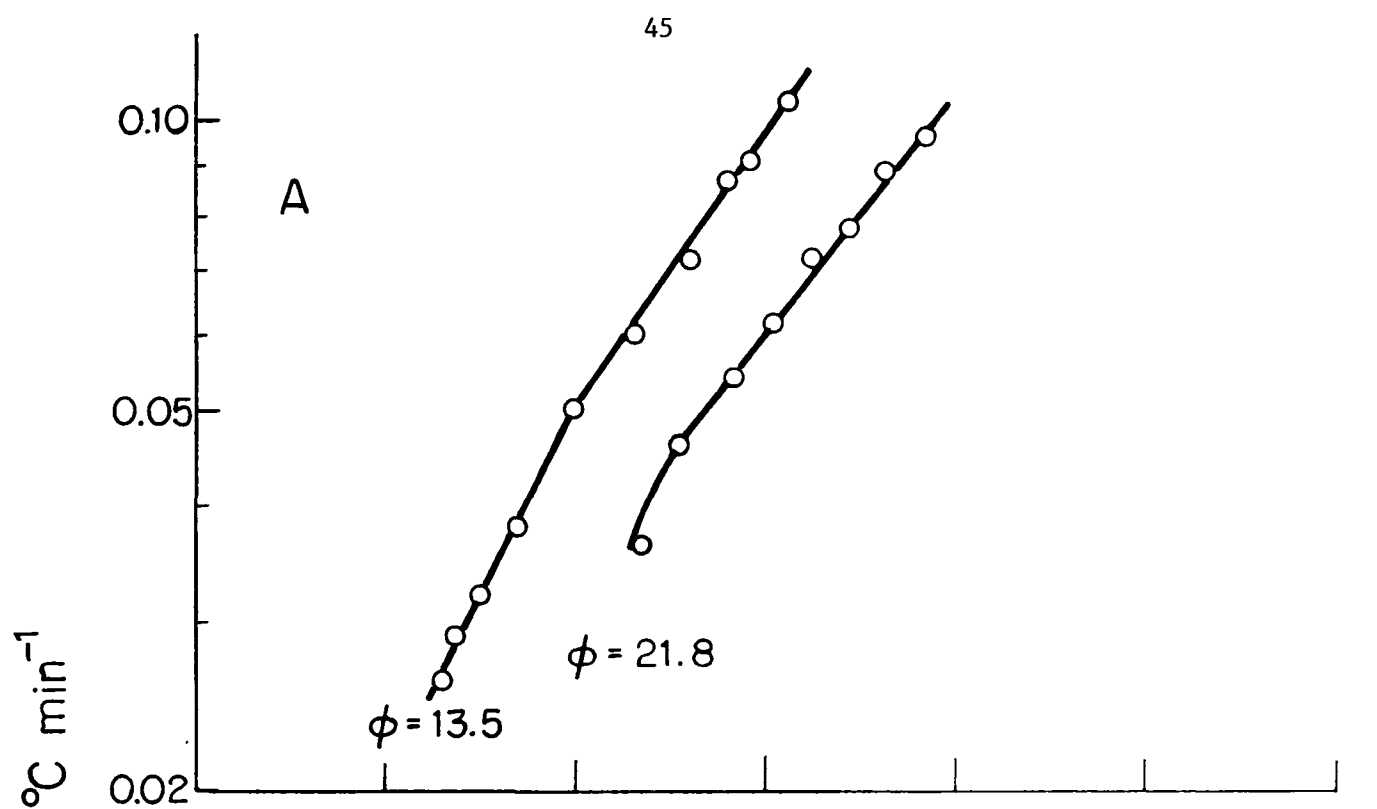


Table 2

Calculation of the activation energy for tetryl
 from the relation between the self-heat rate.
 the temperature and the thermal inertia

Self-heat rate $^{\circ}\text{C mol}^{-1}$	Temperature $^{\circ}\text{C}$		Activation energy kcal mol^{-1}
Titanium bomb			
	<u>$\phi = 13.5$</u>	<u>$\phi = 21.8$</u>	
0.05	140.0	143.5	47
0.07	142.7	146.3	46
0.09	144.5	148.4	43
0.10	145.3	149.3	42
Hastelloy C bomb			
	<u>$\phi = 7.4$</u>	<u>$\phi = 18.7$</u>	
0.05	137.7	143.3	56
0.07	139.7	145.5	55
0.09	141.0	147.5	49
0.10	141.7	148.5	47

The average values, however, are close to those obtained by the other methods for the same bomb.

IV. Evaluation of Techniques

The activation energies calculated from the ARC data by the three methods are in good agreement for a particular bomb, but there is a difference in the values obtained from each type of bomb. This difference may reflect the different thermal conductivity of the bombs, which determines the speed of the response of the system to the heat released by the reaction. In an autocatalytic reaction even small heat losses will have a large effect on the rate of decomposition which in turn determines the rate of change of temperature with time and the value of the activation energy.

The present results are compared with the measurements reported in the literature in Table 3. This Table reveals that the Arrhenius parameters obtained from isothermal techniques are in reasonable agreement, with an average value of 36 kcal mol⁻¹ for the activation energy and 10¹³ sec⁻¹ for the frequency factor. The latter may be considered reasonable for a dissociation involving the breaking of bonds. The techniques involving increasing temperature, including DTA, DSC and ARC, give significantly higher values for the activation energy, the one exception being the work of Hara and Osada [28]. These high activation energies, which were obtained within the temperature range spanned by

Table 3

Measured activation energies for the decomposition of tetryl

Technique	Temperature range °C	Activation energy kcal mol ⁻¹	Frequency factor log A(sec ⁻¹)	Reference
Isothermal	120-140	36.6	12.7	Farmer (18)
Isothermal	211-260	38.4	15.4	Robertson (20)
Isothermal	132-164	34.9	12.9	Cook&Abegg (21)
Isothermal	140-160	35.2	13.5	Dubovitskii et al. (22)
DTA	162	76		Krien (24)
DSC		55		Rogers & Morris (25)
DSC	170-174	58		Hall (26)
Isothermal	140-170	41		Hara & Osada (28)
DTA	170	41.2		Hara & Osada (28)
Isothermal	150-175	35		Hara, Kamei & Osada (27)
Isothermal	180-205	32	13.2	Hutchinson (17)
ARC	140-180	52	21	Present work

The isothermal measurements, do not indicate an exceptionally slow rate for decomposition. They appear to be the result of a very rapid increase in the rate constant with increasing temperature, giving an apparently high value for the activation energy. From the present result the activation energy of 52 kcal mol⁻¹ leads to a frequency factor of 10^{21} s⁻¹. Such a value is impossibly high for a simple dissociation reaction.

It appears that when tetryl is subjected to increasing temperature, the rate of decomposition increases much faster than predicted by a consideration of the Arrhenius energy barrier measured isothermally. A change in mechanism as the reaction proceeds, allowing the occurrence of some steps with lower energy barriers, could cause a strong increase in rate with temperature. This may lead to an apparently high activation energy and a correspondingly high frequency factor, compared to the values measured isothermally. A change in mechanism may occur if products of low stability are formed or if reactive intermediates cause autocatalysis. In such a situation it is surprising that the pseudo first order rate constant appears to follow an Arrhenius behaviour over a wide range of temperature. Nevertheless the empirical activation energy obtained from these experiments cannot be simply interpreted in terms of a particular energy barrier for the decomposition process. The high activation energy coupled with a high frequency factor can probably be taken to

indicate a high sensitivity to autocatalysis and a tendency to undergo a runaway reaction. In this sense the results obtained from techniques using increasing temperature may be valuable in the assessment of thermal hazards.

An early study of the isothermal decomposition of tetryl [18] had reported results which led to high values for the activation energy and frequency factor. These results were subsequently shown [26] to be caused by a large difference in the rate of decomposition between solid and liquid tetryl. A combination of the rate measured in solid and liquid phases gave an apparent activation energy of 60 kcal mol⁻¹ and a frequency factor of 10^{27} sec⁻¹. The reason for the increased rate of decomposition of the liquid has not been adequately explained, but it was concluded that no particular significance could be attached to these values of the activation energy and frequency factor. Since decomposition of tetryl in the ARC occurred after melting, the early results are clearly not related to the measurements obtained in this work.

CHAPTER 6: ANALYSIS OF PRODUCTS

A method for separation and identification of tetryl and related compounds by two dimensional thin-layer chromatography was reported by Yasuda [30].

Positive identification of trinitroanisole was possible through its reaction with sodium ethoxide to form a charge-transfer complex. When sodium ethoxide (0.01-0.1M) is added to 2,4,6-trinitroanisole (10^{-5} M) solution in ethanol at room temperature, a yellow colour is produced immediately. The colour is the result of absorption by a charge-transfer complex formed between TNA and sodium ethoxide [31,32].

In the present study, both thin-layer chromatography and UV-VIS absorption spectroscopy were used in the separation and identification of the products.

I. Materials and Apparatus

Tetryl used in this study was from Defence Research Establishment, Valcartier, Que.(DREV), and used without further purification. Sodium ethoxide solution, 0.1M, was prepared by dissolving sodium ethoxide, 97% (Aldrich Chemical Company), in ethanol. Picric acid, ACS grade, was obtained from Anachemia Chemical Company and a standard solution of 100 ppm was prepared and used in further dilutions. A standard tetryl solution, 100 ppm, was also prepared. All solvents were reagent grade.

Pre-coated TLC plates, Silica Gel 60F-254, with layer thickness 0.25 mm, were obtained from Canadawide Scientific Co.

The UV-VIS spectroscopic analysis of the decomposition products was performed using a Shimadzu Model 200UV double-beam spectrophotometer with 1 cm cells and 1 nm slit width.

1J. Procedure

Tetryl was decomposed in the ARC according to the procedure described in chapter 3 using a 0.15 gram sample in the Titanium spherical bomb with the 3/16" x 1" tube stem. Instead of continuing the decomposition until completion, the reaction was stopped at a pre-selected temperature and cooled immediately. In this way products were collected and analyzed at various stages during the reaction.

(a) Collection of the Samples

After cooling, the sample was dissolved in ethanol and transferred to a volumetric flask. The spherical bomb was rinsed with ethanol until the solution was colourless. Because complete removal with ethanol was difficult, acetone was used to dissolve any remaining solids. The acetone solution was transferred into a beaker and air dried. What remained was dissolved with ethanol, combined with the first ethanol solution and diluted to volume. If a residue was present, the weight was determined by the weight difference of a filter paper before and after filtering the final

ethanol solution. After air drying of the bomb, it was weighed to check for complete removal of the sample. The weight loss after reaction was determined from the difference in weight before and after reaction.

(b)_Analysis_of_Products

The two major products which have been reported from the decomposition of tetryl are trinitroanisole and picric acid. Analysis for the former product was considerable hindered by the inability to obtain a sample of trinitroanisole, due to restriction on its sale. Nevertheless by a combination of TLC analysis and UV-VIS spectrophotometric analysis and making use of published values for the absorption coefficient for trinitroanisole, a quantitative analysis for the reaction products was obtained.

(c)_Thin-layer_Chromatography_Analysis

TLC technique was used successfully in separation and identification of the decomposition products. The solution containing the decomposition products was applied on two silica gel TLC plates. Each plate was developed in benzene and a solution of benzene/methanol/acetic acid (90/16/8 by volume) for 10 cm and air dried. Three components of the mixture were observed, of which bands 2 and 3 were identified as tetryl and picric acid respectively, by comparison of retention times of the pure compounds. The relative retention time (R_f) values are summarized in Table 4. A better separation was achieved using benzene as developer and it was used in subsequent measurements.

Table 4

R values of tetryl, picric acid and thermal decomposition
 f products mixture

Developing solvent	Sample/R f		
	<u>Tetryl</u>	<u>Picric acid</u>	<u>Decomp. products</u>
Benzene	0.26	0.00	(1) 0.45
			(2) 0.26
			(3) 0.00
Benzene/methanol/ acetic acid, by vol. (90/16/8)	0.64	0.23	(1) 0.73
			(2) 0.65
			(3) 0.23

Further identification of the components of the mixture was made by recovery of the separated bands on the TLC plates. Two ml of the ethanol solution was used for the separation. After development in benzene followed by air drying, each band, 1 cm width, was scraped off and extracted 5 times, using 5 ml of ethanol each time. The extracts were centrifuged, combined and diluted to 25 ml. A plate was treated in the same way using the pure solvent to serve as blank.

(11) UV-VIS Spectrophotometric Analysis

Calibration curves for tetryl and picric acid were obtained using ethanol solutions of 20, 15, 10, 5 and 4 ppm, prepared from the stock solution of 100 ppm. Each solution was scanned from 800 to 200 nm. For tetryl the absorption maximum was at 230 nm, while picric acid showed maxima at 215 nm and 360 nm. Figure 7 shows the spectra of tetryl, picric acid and trinitroanisole in ethanol solution. A linear relation between absorbance and concentration was obtained for tetryl and picric acid at the wave lengths shown in Table 5, where the values for the absorption coefficients are given. The absorbance of mixtures of tetryl and picric acid at the wavelengths indicated may therefore be expressed by the following equation.:

$$A_{400} = 53 [\text{picric acid}] \quad (15)$$

Figure 7

Absorbance as a function of wavelength, individual compound
in ethanol solution

△ : tetryl, 10 ppm

● : picric acid, 10 ppm

□ : trinitroanisole, 2.4 ppm

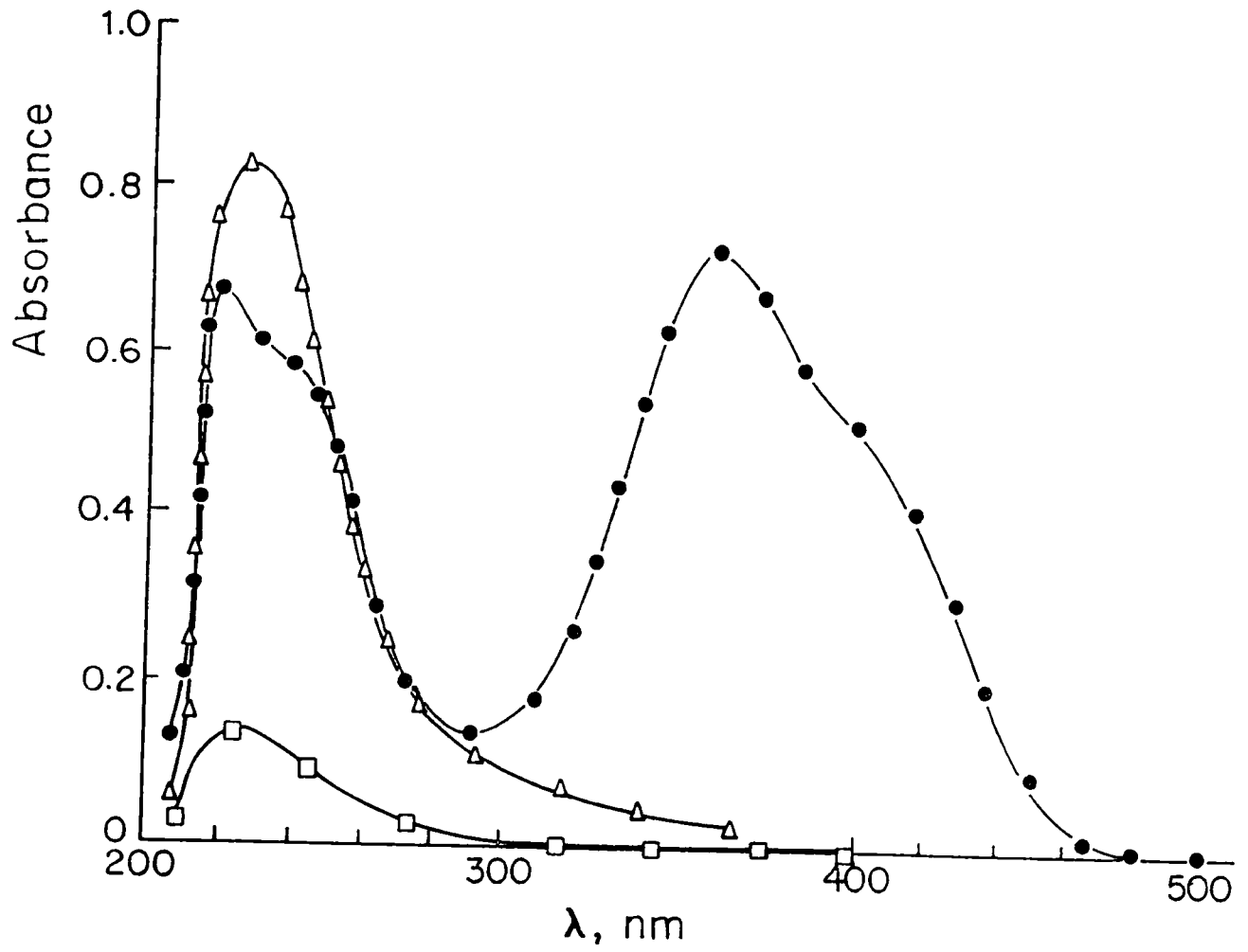


Table 5
Absorbance of solutions of tetryl and picric acid

Compounds	Wavelength nm	Concentration g L ⁻¹					a L g ⁻¹ cm ⁻¹
		<u>0.020</u>	<u>0.015</u>	<u>0.010</u>	<u>0.005</u>	<u>0.004</u>	
Tetryl	230	1.52	1.18	0.82	0.41	0.32	81
Picric acid	230	1.24	--	0.62	0.30	0.25	62
	400	1.06	--	0.52	0.26	0.21	53

$$A_{330} = 62 [\text{picric acid}] + 81 [\text{tetryl}] \quad (16)$$

where the concentrations are expressed as g L^{-1} .

The absorbance of mixtures of tetryl and picric acid was measured to confirm that no chemical interaction occurred under the condition of the measurements.

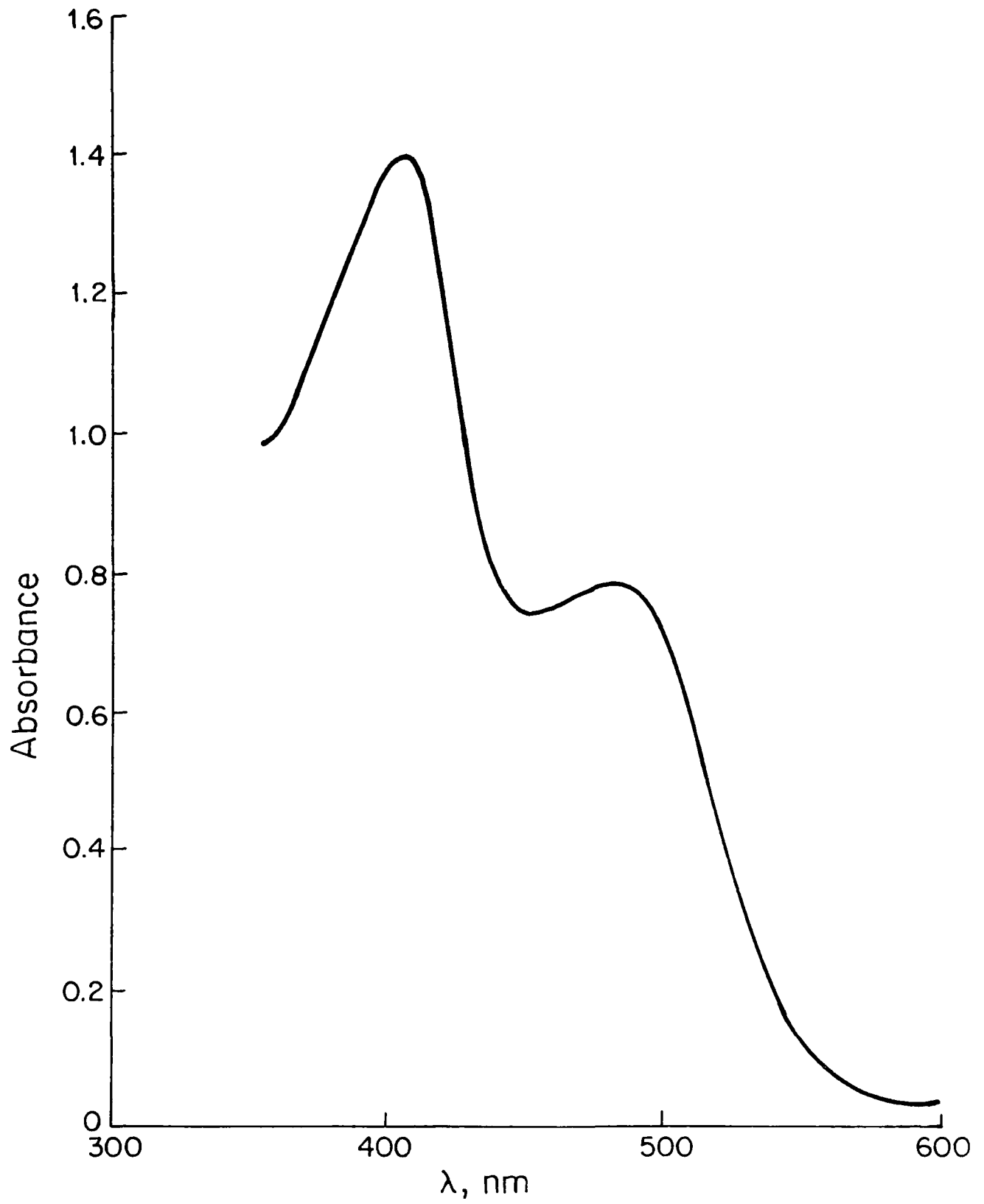
Measurements were made with equal volume mixtures of various concentrations of tetryl and picric acid solutions. The concentrations of the mixtures were calculated from the measured absorbance using equations (15) and (16). Table 6 shows good agreement between the predicted and measured concentrations of the mixtures, confirming that no interaction occurs.

Identification of bands (2) and (3) from the TLC separation as tetryl and picric acid respectively, was confirmed by the individual spectra. Identification of band (1) as trinitroanisole was made through its reaction with sodium ethoxide solution to form the σ -complex with strong absorption maximum at 410 nm and 490 nm [31,32]. Band (1) reacted with 0.1 M sodium ethoxide solution in ethanol. The spectrum of this solution, the σ -complex of TNA, is shown in Figure 8. The concentration of trinitroanisole was determined using the published value for ϵ at 490 nm ($15850 \text{ L mol}^{-1} \text{ cm}^{-1}$) [33], where the other products do not absorb, from the following equation:

Table 6
 Concentrations of equal volume mixture
 of Tetryl and picric acid

Prepared mixtures concentration g L^{-1}		Measured absorbance		Calculated concentration g L^{-1}	
<u>Tetryl</u>	<u>P.A.</u>	<u>λ_{400}</u>	<u>λ_{230}</u>	<u>Tetryl</u>	<u>P.A.</u>
0.0025	0.0075	0.38	0.64	0.0024	0.0072
0.0050	0.0050	0.26	0.70	0.0048	0.0050
0.0025	0.0050	0.25	0.52	0.0037	0.0048
0.0050	0.0025	0.13	0.55	0.0048	0.0025
0.0025	0.0025	0.13	0.38	0.0027	0.0025
0.0020	0.0020	0.10	0.27	0.0017	0.0021

Figure 8
Absorbance as a function of wavelength for σ -complex of
trinitroanisole in ethanol solution
solution of TNA, 24 ppm and sodium ethoxide, 0.1M



$$A_{490} = 65 [\text{TNA}] \quad (17)$$

where a is expressed in units of $\text{L g}^{-1} \text{cm}^{-1}$ and the concentration of TNA is given as g L^{-1} .

Analysis of the condensed-phase products by these methods was made after stopping the reaction at selected temperatures throughout the course of the reaction. In some cases the recovered solution was not separated into the component fractions. From the spectrum of the solution containing all the products, only the concentration of picric acid could be determined. The absorbance at 400 nm is due to picric acid only (see Figure 7). In these experiments the weight loss was measured in the usual way.

CHAPTER 7: PRODUCTS, MECHANISM OF THE THERMAL DECOMPOSITION
OF TETRYL

1. Condensed-phase Decomposition Products of Tetryl

The main condensed-phase products previously reported from the decomposition of tetryl, trinitroanisole and picric acid [23,28,30], were detected and analyzed in the decomposition under the present conditions. The products were measured at various stages in the decomposition in the ARI and the results are presented in Table 7 and Figure 9. The kinetic features of the decomposition are in essential agreement with the results of Dubovitskii and co-workers [22,23] and of Hara and Osada [28]. These independent studies both led to the conclusion that trinitroanisole and picric acid were both primary products, formed by parallel routes, and that trinitroanisole subsequently decomposed to picric acid, which in turn decomposed at higher temperatures. This interpretation was most evident from the isothermal decomposition but was also supported by the DTA experiments of Hara and Osada [28] in which three exothermic peaks were observed. These peaks were identified with the sequential decompositions described above. Examination of Figure 9 shows that both TNA and picric acid are formed at the beginning of the reaction and are probably both primary products. TNA was less stable than picric acid and its maximum yield was achieved at about 160 °C whereas the maximum yield of picric acid was at about 190 °C.

Table 7

Condensed-phase products from the decomposition of tetryl
in the ARC

Temperature °C	%TNA	%Picric acid	%Tetryl	%Wt. loss	%Residue ethanol insol.
150	20.1	12.1	59.8	8.0	0
155	NA	24.9	NA	13.3	0
160	39.4	26.3	15.6	18.7	0
165	36.1	26.5	18.9	18.5	0
180	15.4	46.5	0.5	25.9	11.7
185	NA	49.0	NA	29.2	NA
200	4.4	41.2	0.7	38.5	15.2
217	NA	22.3	NA	48.1	NA
254	NA	0.03	NA	67.1	NA

NA not available

Figure 9

Self-heat rate, A, reactant and product composition, B,
as a function of $1/T$. Ti bomb; $\phi = 21$

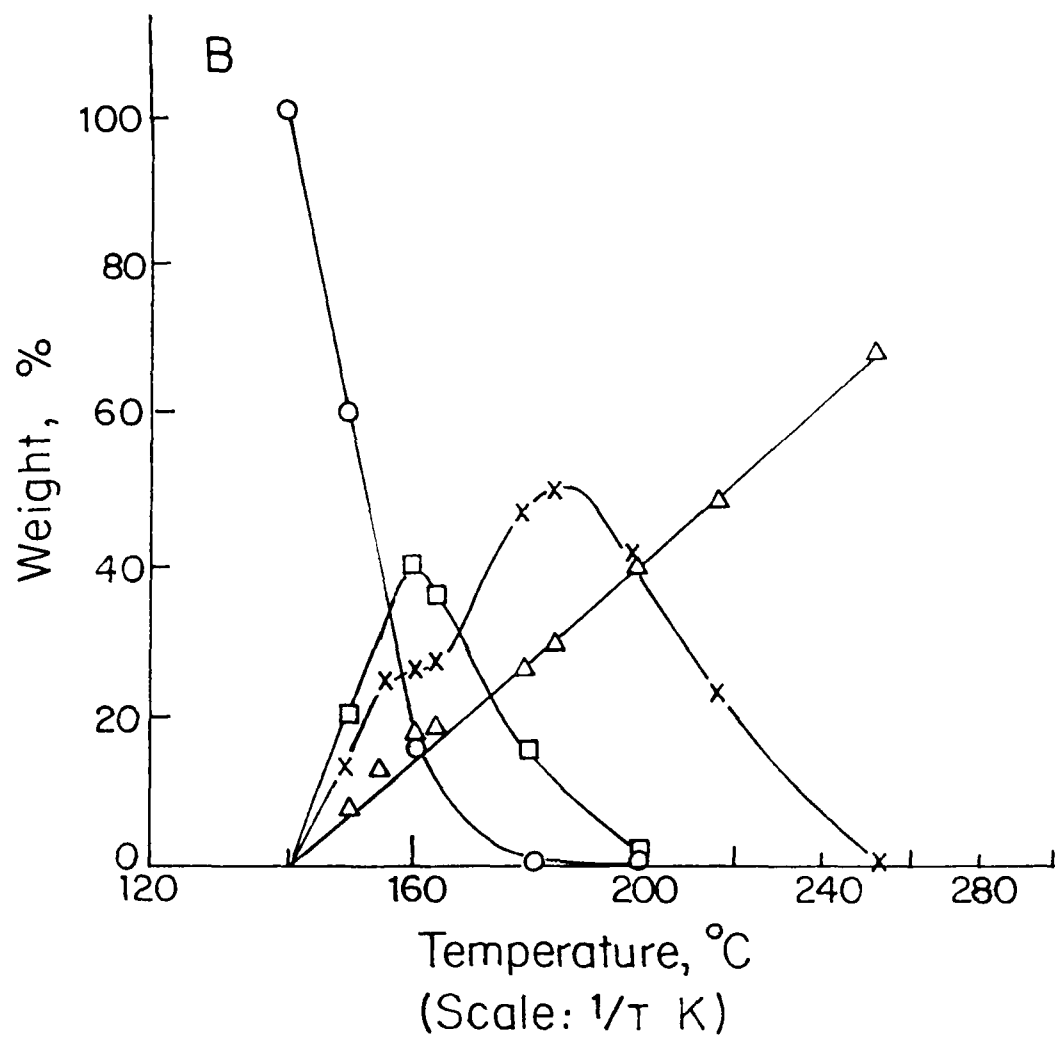
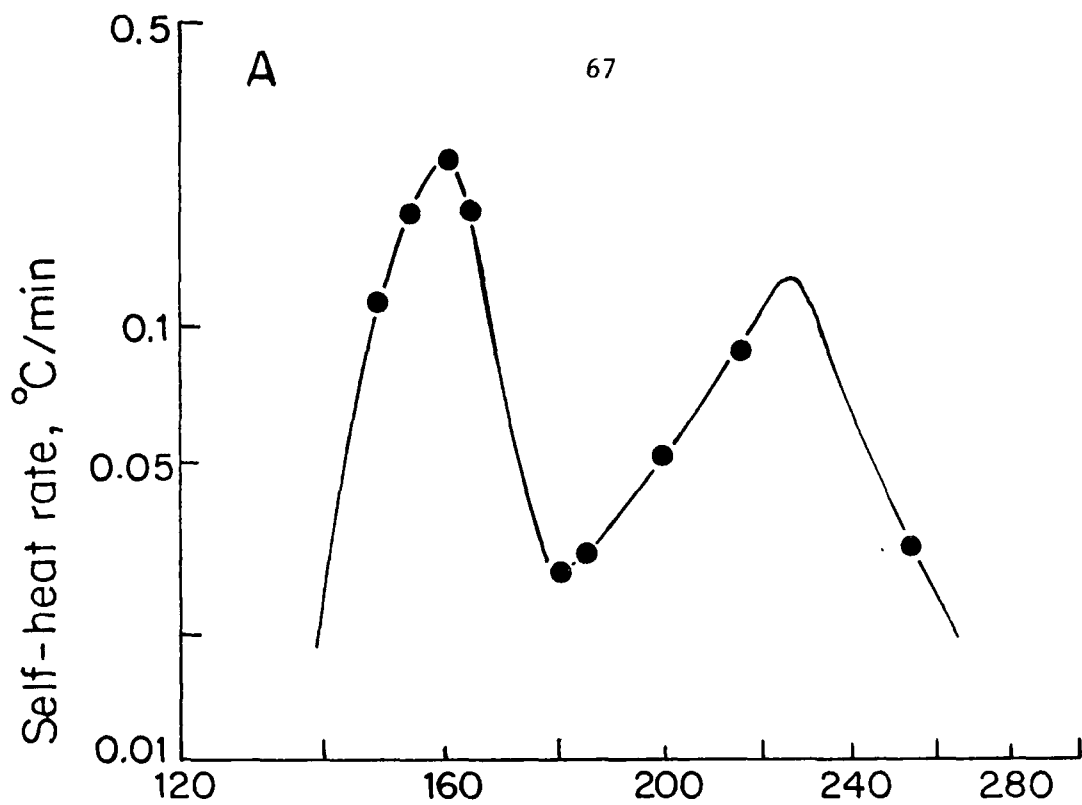
A. Points indicate the temperature at which reaction was
stopped for analysis

B. O: tetryl

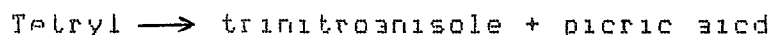
□: trinitroanisole

X: picric acid

Δ: weight loss, $w_o - w_f$



In contrast to the DTA results, the self-heat rate measured in the ARC shows only two well-defined peaks with increasing temperature. By comparison with the composition of the products as shown in Figure 9, the first correlated with the disappearance of tetryl into both picric acid and trinitroanisole. The temperature at the maximum rate was 161 °C where only about 15% of the tetryl remains. The rate constants obtained through analysis of the first peak therefore relate to the over-all decomposition of the tetryl. The conversion of trinitroanisole into picric acid, evident from the analysis shown in Figure 9B, is detectable only as an asymmetry in the first peak in Figure 9A, although data obtained using a larger amount of tetryl showed a small shoulder on this curve. The minimum between the peaks corresponds to complete disappearance of tetryl and the value of ΔT should therefore give a reasonable value for ΔH of the reaction.



The beginning of the second peak, 180 °C to 200 °C, refers to the decomposition of the remaining 10% of trinitroanisole into picric acid and the decomposition of picric acid. The major part of the second peak describes the decomposition of picric acid and the maximum rate (not as well-defined as for the first peak) occurs at about 228 °C.

at which temperature about 20% of the maximum amount of picric acid remains. Kinetically these two peaks may be considered as separated, and each analyzed independently. The difference in temperature between the points of maximum rates for each decomposition was about 65 °C, but this difference will be a function of the rate and the ΔH of each decomposition and is not a general criterion for separation.

II. Mechanism of the Decomposition

From the measurements of k as a function of temperature for the first decomposition peak, values of the activation energy, 52 kcal mol⁻¹ and the frequency factor, 10^{31-23} sec⁻¹, were obtained and reported in chapter 5. It was suggested in this chapter that these "high" values, which cannot be interpreted in terms of passage over an energy barrier in the usual way, were the result of changes in the mechanism of decomposition as the reaction proceeds. Arrhenius parameters were also derived by kinetic analysis of the measurements of the second decomposition peak. Although less reliability is achieved from these measurements, it is evident from Table 1 that the activation energy, of about 40 kcal mol⁻¹, is lower than that obtained from the first peak. With this activation energy and the measured value of k (Figure 4), a value for the frequency factor in the range 10^{13-15} sec⁻¹ was obtained. This decomposition therefore has Arrhenius parameters which are closer to those expected

for a bond-breaking process. From Figure 9 it appears that this decomposition begins only after tetryl has completely disappeared and trinitroanisole has almost disappeared. The self-heat rate therefore describes the decomposition of picric acid and the Arrhenius parameters obtained are in reasonable agreement with those reported previously for picric acid ($E = 38.6 \text{ kcal mol}^{-1}$, $A = 4.10 \times 10^{11} \text{ sec}^{-1}$) [34,35].

In all studies of the decomposition of tetryl, reference is made to the autocatalytic character of the reaction. In several studies [29], it was suggested that picric acid may catalyze the decomposition of tetryl, possibly by a proton transfer reaction, giving a cation which is considerably less stable than the molecule. This conclusion is largely based on the results of the experiments of Hinshelwood [19] and of Dubovitskii and co-workers [22,23] in which addition of picric acid increased the rate of decomposition of tetryl and removed the induction period. The present results and those of Hara and Osada [28], as discussed in their work, do not substantiate this role of picric acid. The results of the isothermal decompositions at 150 °C reported by Hara and Osada suggest that autocatalysis occurs before the formation of trinitroanisole and picric acid. The decomposition was not accelerated by either of these products. The results shown in Figure 9, although not as extensive as the isothermal results, also do not indicate

a particular acceleration of the decomposition by the formation of picric acid. This conclusion suggests that the increase in rate on addition of picric acid may be associated with the lowering of the melting point, as recognized by Hinshelwood [19] and discussed by Hall [26].

The more probable cause of autoacceleration is the formation of the reactive products, nitrogen dioxide and nitric oxide. The analysis of the gaseous products reported by Dubovitskii and co-workers [22,23] showed that both nitrogen dioxide and nitric oxide disappeared in secondary reactions and these authors recognized the importance of these reactive radicals in promoting decomposition of tetryl. Reactive gaseous products may exert their effect before diffusion from the solid phase. The effectiveness of this autocatalysis may therefore depend on a number of factors, such as the efficiency of removal of the products from the decomposing solid. Decomposition during increasing temperature may be more critically affected by the presence of these products.

In summary, the two peaks in the self-heat rate as a function of temperature observed in the decomposition of tetryl in the ARC are shown to relate to the simultaneous decomposition into trinitroanisole and picric acid and to the subsequent decomposition of picric acid, respectively. From the kinetic analysis of the self-heat rate for the first peak, a "high" activation energy and frequency factor were

obtained, suggesting a complex mechanism of decomposition, probably involving autocatalysis. The kinetic parameters obtained from the analysis of the second peak are "normal" for a decomposition process and in agreement with previous results.

CHAPTER 8: NITROGUANIDINE

I. Properties

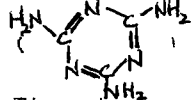
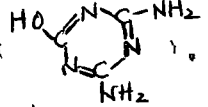
Nitroguanidine is an important ingredient in triple base propellants. It exists in two forms, α and β , with densities 0.3 g cm^{-3} and $0.9\text{-}1.0 \text{ g cm}^{-3}$ respectively. Both forms of nitroguanidine melt at the same temperature, $232 \text{ }^\circ\text{C}$, although higher melting points, $246 \text{ }^\circ\text{C}$ and 257°C , have been reported [16]. DTA studies of Ripper and Krien [36] suggested that the α form begins to decompose at $187 \text{ }^\circ\text{C}$, while the β form decomposes at $205 \text{ }^\circ\text{C}$. Many tests concerning the properties of nitroguanidine were performed by the U.S. Army Material Command [37].

II. The Thermal Decomposition of Nitroguanidine

From the thermal decomposition of nitroguanidine in the range $190\text{-}240 \text{ }^\circ\text{C}$, the main gaseous products are N_2O , H_2O , NH_3 and CO , accompanied by a large quantity of solid products. A mechanism involving two pathways has been proposed [38]. The first decomposition pathway involved nitramide (NHNO_2) and cyanamide (NH_2CN) as intermediates, while nitrocyanamide (NQNH_2CN) was the intermediate from the second pathway. Stals and Pitt discussed the structure and reactivity of nitroguanidine and concluded that intramolecular hydrogen bonding was stronger than intermolecular hydrogen bonding. The primary reaction pathways in the thermal decomposition of

nitroguanidine are therefore predominantly intramolecular.

Studies of the decomposition by thermoanalytical techniques showed that a single exothermic maximum occurred at 150 °C [39] while a thermogravimetric study [40] showed that the initial weight loss began at 220 °C. Rogers [41,42] measured an activation energy for decomposition by the DSC technique of 21 Kcal mol⁻¹.

Volk [43] identified the solid products and analyzed the gaseous products of nitroguanidine decomposition by mass spectrometry. He found that N₂O and NH₃ were the main gaseous products and their ratio was temperature dependent. The solid residue at 130 °C, melamine () and ammeline (), was analyzed using HPLC. The decomposition behaviour was strongly affected by the confinement. Up to 60-70% weight loss occurred during decomposition. The residue contained mainly melamine and ammeline and was considerably heat resistant. From the measurements of the rate of weight loss, an activation energy of 51.6 Kcal mol⁻¹ was obtained.

Taylor and Andrews, Jr. [4] used the flowing-afterglow spectroscopy technique to study the solid phase thermal decomposition reaction. NH₃, N₂O, CO and H₂O evolved from nitroguanidine were analyzed by monitoring the emission of NH₃^{*}, OH^{*}, N₂O⁺ and CO₂⁺. The activation energies were calculated from the slopes of the curves, log rate as a function of 1/T. These measurements led to high activation

energies (70-110 Kcal mol⁻¹) and correspondingly high frequency factors (10³⁰⁻⁵⁰ sec⁻¹). They suggested that this result may be due to autocatalytic evolution of gases which led to violent decomposition above 160 °C. After this phenomenon occurred once, the activation energy became 25-25 Kcal mol⁻¹ and frequency factor was 10⁵⁻⁷ sec⁻¹. These values are more typical of organic thermal degradation.

Few studies of the kinetics of the decomposition have been attempted. Because of the complexity of the reaction, the kinetic parameters which have been reported are very difficult to interpret in terms of the mechanism of the decomposition. The present work describes some preliminary experiments on the decomposition of nitroguanidine in the ARC, primarily for the purpose of obtaining kinetic parameters for the decomposition. The effects of sample size and confinement of gaseous products have been investigated.

1.1.1. Experimental

The thermal decomposition of nitroguanidine was studied using the Hastelloy C spherical bomb with the filler tube of 3/16 inch O.D. and 1/2 inch length. The experiments were performed in both the confined and non-confined systems. The thermal inertia ranged from 15 to 22, obtained by using weights of sample between 0.2 and 0.3 grams. Experiments were performed using the heat-wait-search method described in Chapter 3.

IV. Results

A. General Features

When nitroguanidine was tested in the confined system, the decomposition commenced between 161 and 165°C depending on the value of the thermal inertia. The ignition rate was not vigorous, the time to maximum rate was short, and pressure build-up was fast. The results are summarized in Table 8 and the self-heat rate and pressure as a function of $1/T$ are plotted in Figure 10. The total adiabatic temperature rise was in the range of 15-17 °C depending on the value of ϕ . After reaction, the percent weight loss was approximately 65%. The high amount of residue may have been due to inhibition of the products to further decomposition [43].

When nitroguanidine was tested in the non-confined system, the reaction stopped after a short period of time. The onset of decomposition was detected at about 200 °C. The self-heat rate was slow and the adiabatic temperature rise only 2-3 °C. Experimental results indicated that the decomposition behaviour was strongly dependent on the confinement. This phenomenon suggested that the decomposition of nitroguanidine was sensitive to pressure and decomposition products.

B. Calculation of the Activation Energy

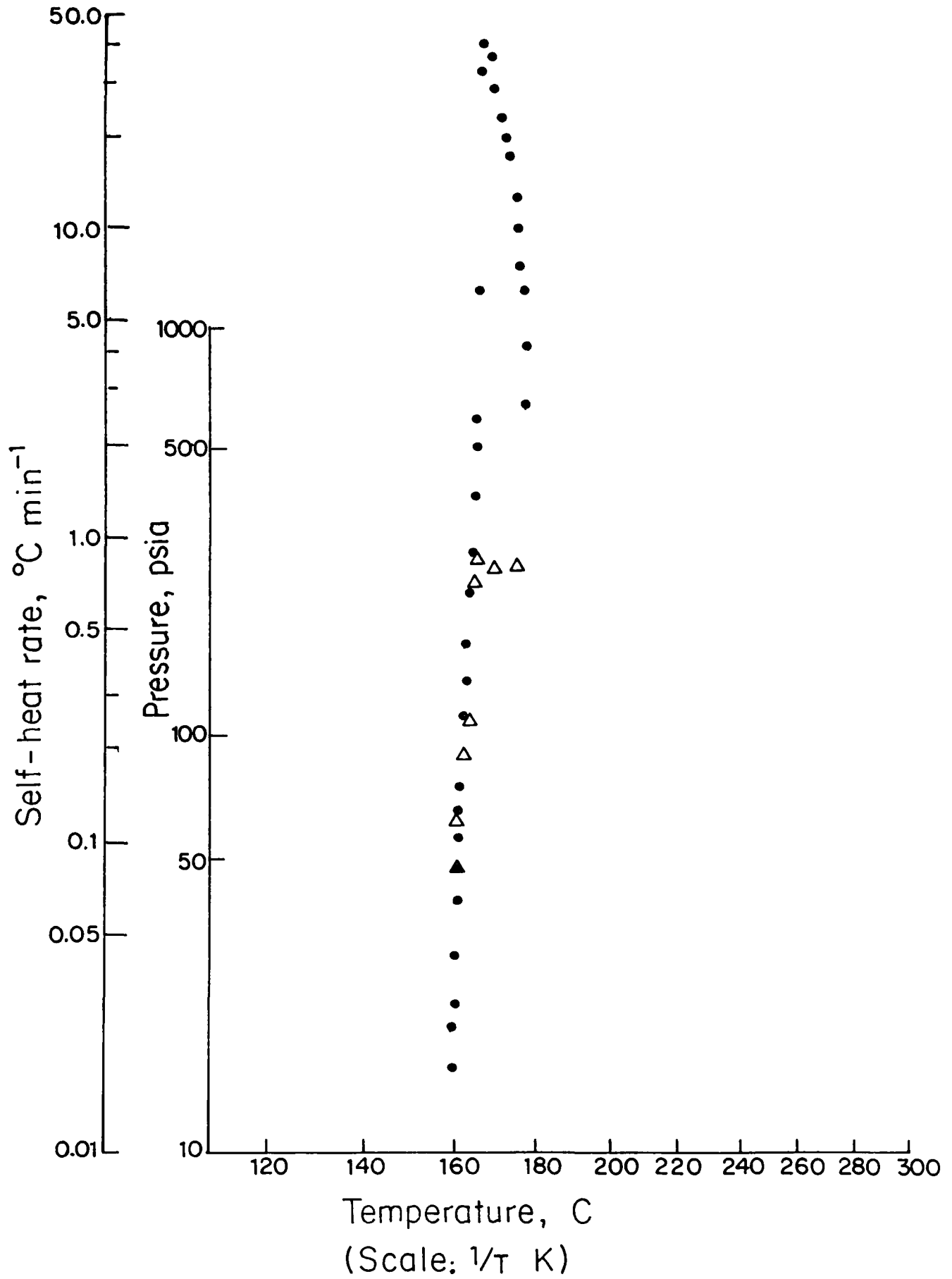
In this study, the activation energy of decomposition of nitroguanidine was calculated following the

Table 8

Thermal decomposition data of nitroguanidine

Expt#	Weight	ϕ	T_o	m_o	T_m	m_m
	η		$^{\circ}\text{C}$	$^{\circ}\text{C min}^{-1}$	$^{\circ}\text{C}$	$^{\circ}\text{C min}^{-1}$
Confined_system						
165	0.2135	20.9	165.9	0.04	172.4	28.5
166	0.2540	17.7	161.0	0.02	170.1	21.0
231	0.2362	19.6	161.7	0.04	168.9	44.5
349	0.2328	21.2	166.6	0.09	175.2	10.8
350	0.2541	18.6	160.9	0.03	167.3	30.5
328	0.3074	15.1	160.9	0.03	171.2	25.5
329	0.2068	22.1	167.6	0.32	173.3	15.0
Non-confined_system						
169	0.2348	19.1	198.7	0.04	201.7	0.06
170	0.2433	18.5	202.0	0.07	204.6	0.12

Figure 10
Self-heat rate, ●, and pressure, Δ, as a function of $1/T$
for nitroguanidine. Hastelloy C bomb; $\phi = 19.6$



Three methods which were derived by Townsend and Tou [5] and discussed in Chapter 5. The experiments in the non-confined system had very short therms which did not provide enough data for the determination of the activation energy. Only the data from the confined system was analyzed.

(a) Calculation from k^*

The estimation of the Arrhenius parameters from the plot of the k^* against $1/T$ was the simplest approach, since the curve was plotted automatically from the microprocessor of the ARC. In the decomposition of nitroguanidine, the self-heat rate increased very rapidly, giving a very steep slope and hence a high activation energy, approximately $300 \text{ Kcal mol}^{-1}$. This very high value led to an impossibly high value for the frequency factor.

(b) Calculation from Time to Maximum Rate

The relationship between the time to maximum rate and the absolute temperature (equation 13, p.40) was discussed in Chapter 5. The time to maximum rate was plotted as a function of $1/T$ and a typical result is shown in Figure 11. The slope was determined by linear regression. The activation energies determined by this method were in agreement with those obtained from method (a), about $300 \text{ Kcal mol}^{-1}$. The frequency factor was also correspondingly high.

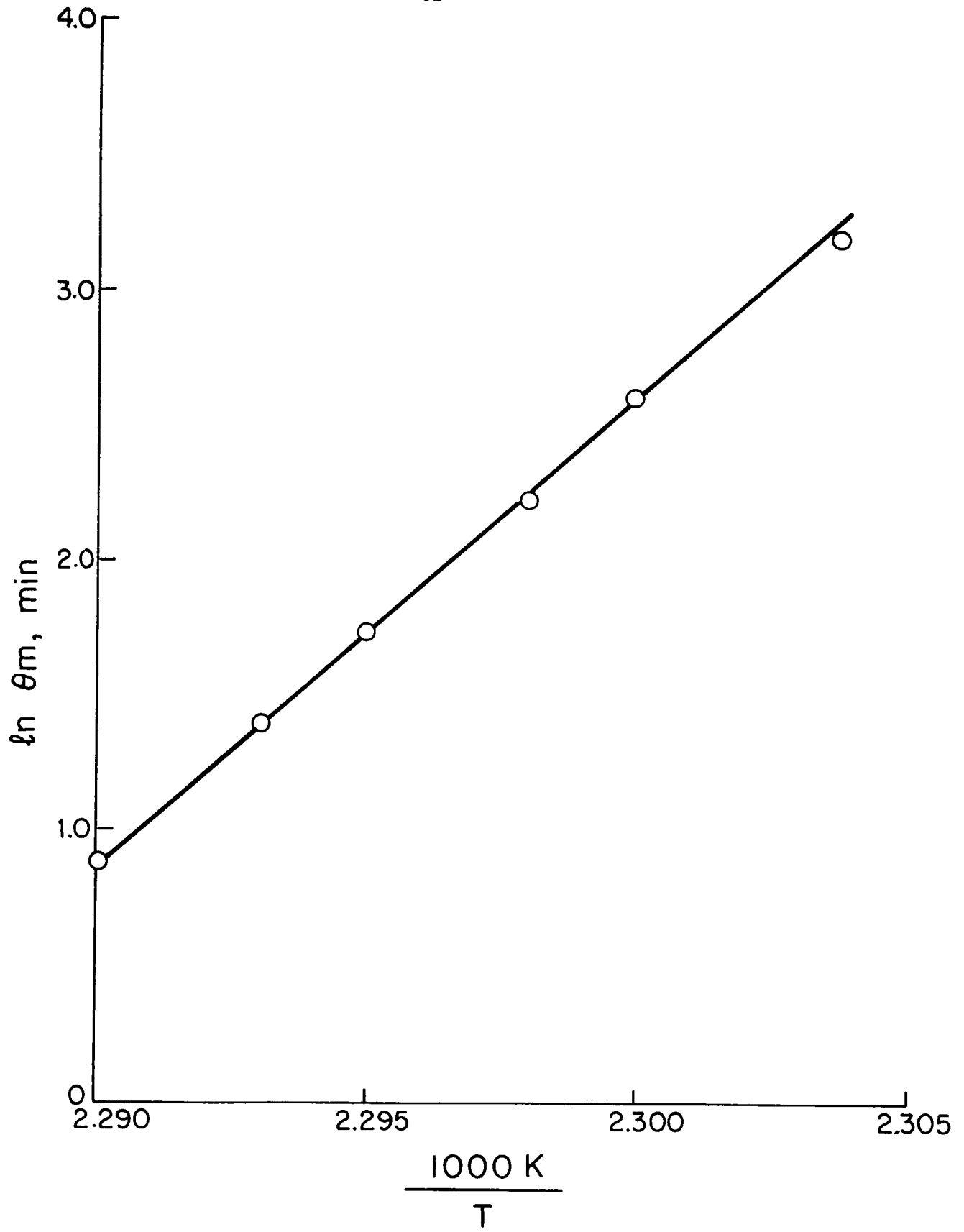
(c) Calculation from the Initial Rate

For determination of the activation energy by method (a) and (b), data from the complete course of the

Figure 11

Time to maximum rate as a function of $1/T$ for nitroguanidine.

Hastelloy C Bomb: confined system; $\phi = 18.6$



reaction were used. The results demonstrated that these treatments did not give reasonable values for an activation energy and frequency factor for the decomposition of nitroguanidine. The third method used data only from the initial stages of the reaction.

The relationship between temperature, thermal inertia and activation energy was given by equation 14. p.43. For this method temperatures are determined at which the self-heat rates are the same for experiments with different values of ϕ . For the most accurate measurement of these temperatures, the self-heat rate is plotted as a function of temperature for each experiment, as described in Chapter 5. Two of these plots are shown in Figure 12. Temperatures were measured at self-heat rates of 0.05, 0.07, 0.09 °C min⁻¹, and the values given in Table 9. The activation energy was then obtained from equation 14 and the values included in Table 9. The average value was 32±2 kcal mol⁻¹.

Nitroguanidine is a very fluffy material with low density. Heat transfer in this solid may not be uniform, causing a certain degree of difficulty in obtaining reproducible data. This factor could cause further uncertainty on the value obtained for the activation energy of this decomposition.

Figure 12

Self-heat rate as a function of temperature for various values of θ for nitroguanidine. Hastelloy C bomb

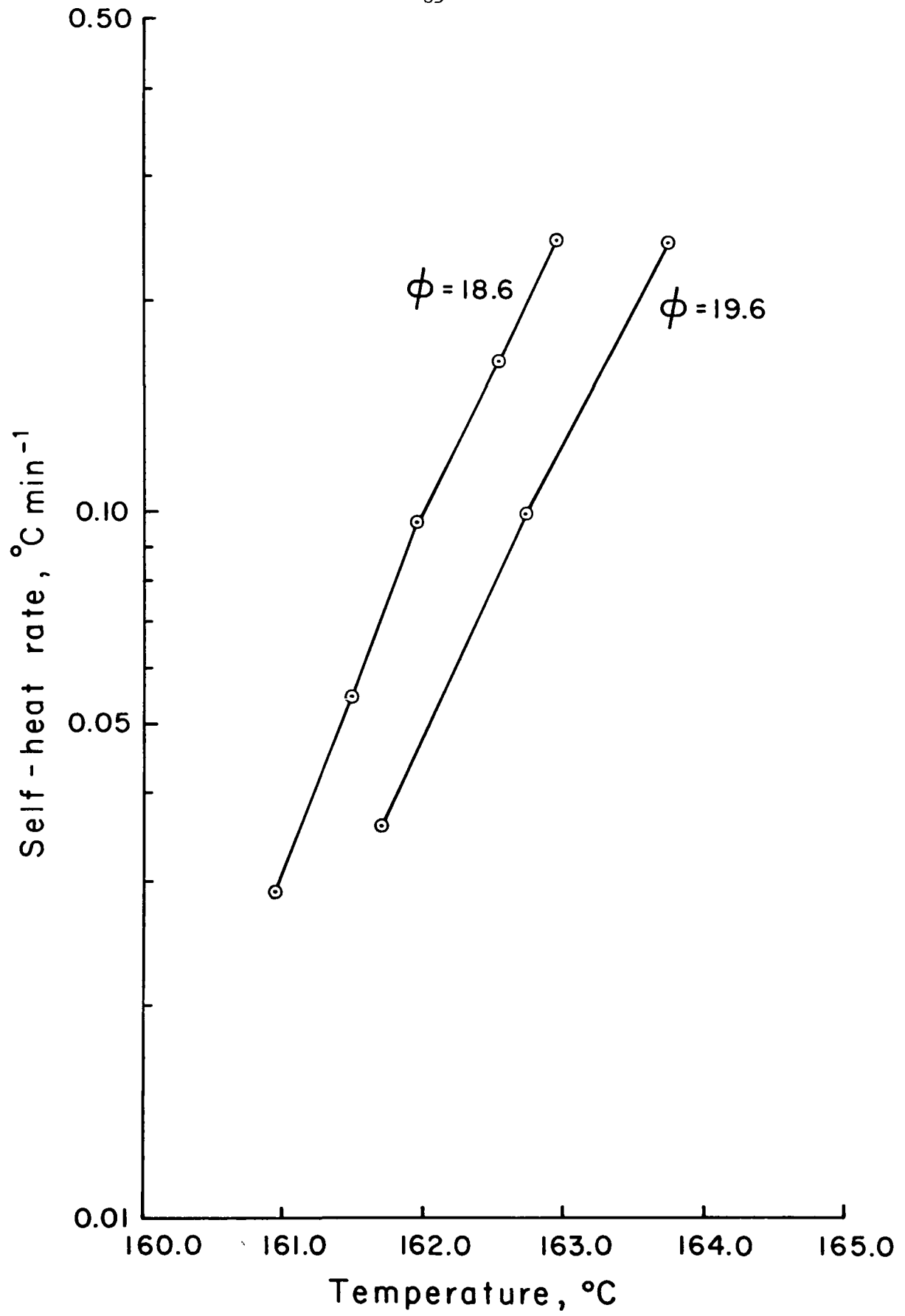


Table 9

Calculation of the activation energy for nitroguanidine
 from the relation between the self-heat rate,
 the temperature and the thermal inertia

Self-heat rate	Temperature		Activation energy
$^{\circ}\text{C min}^{-1}$	$^{\circ}\text{C}$		kcal mol^{-1}
	<u>$\phi = 18.6$</u>	<u>$\phi = 19.6$</u>	
0.05	161.40	162.00	34
0.07	161.70	162.30	34
0.09	161.90	162.55	29

V. Interpretation of the Activation Energy

The activation energy for the decomposition of nitroguanidine calculated from the ARC data by method (a) and (b) gave high values of about $300 \text{ kcal mol}^{-1}$ with correspondingly high frequency factors which cannot be explained by a simple bond-breaking mechanism. On the other hand, the activation energy determined by method (c), which involved only measurements at the initial stages of the decomposition was a reasonable value for the rearrangement of an unstable compound.

The very high values of $300 \text{ kcal mol}^{-1}$ are more difficult to explain. These values were obtained using data covering the whole course of the decomposition and involving a change in temperature as well. During this process some reactions occur which increase the rate enormously and continuously. Empirically, the result suggests a series of steps occurring with progressively lower energy barriers. A possible route to this effect could be autocatalysis, caused by reactive intermediates. The difference in rates obtained in the confined and non-confined systems suggests reactive intermediates may be important.

Comparing the melting point of nitroguanidine reported by other authors [16,36] to the temperature of the onset of decomposition, 161°C detected by the ARC, it appears that nitroguanidine decomposes in the solid state. A solid state decomposition is usually a slow process until some change

allow its decomposition rate to increase sufficiently for it to self-heat to explosion. The decomposition rate of a solid can also vary tremendously with changes in purity and crystal perfection and is affected by other factors, such as, the rate of nuclei formation and the strains created by the new solid phase. All these occurrences lead to complications which could contribute to the unusually large increase in rate observed over the course of the decomposition. These and other factors have been discussed recently in a review of processes occurring during the thermal decomposition of solids by Boldyrev [44].

When the temperature increase in the bomb is very fast, there may be insufficient time for the bomb and the sample to come to thermal equilibrium. This may cause the measured temperature to be lower than the temperature of the sample. It should be pointed out that if the temperature of the bomb and the sample are not equilibrated, as may happen when the temperature increase is very fast, the measured rate of decomposition will be too slow. This error therefore is not a factor contributing to the fast rates of decomposition observed with nitroguanidine.

The results of the present work are compared with the kinetic parameters cited in the literature in Table 10. The experiments by DSC and the second stage of the experiments by the flowing-afterglow techniques indicated low values for the activation energy, comparable to the value obtained in the

Table 10
 Measured activation energies for the decomposition of
 nitroguanidine

Technique	Temperature range °C	Activation energy kcal mol ⁻¹	Frequency factor log A(sec ⁻¹)	Reference
Flowing-	160-180	70-110	30-50	Taylor &
afterglow	160	25-35	5-7	Andrew Jr. (4)
Isothermal	110-240	51.6	21.2	Volk (43)
DSC	200-204	20.9	7.5	Rogers (41)
ARC	160-180	~300		Present work
	160-168	32		Present work

present work from the data at the initial stage of the decomposition. On the other hand, a first stage in the decomposition was observed in the flowing-afterglow experiments where a very rapid reaction occurred, described by the authors as "virtually catastrophic". Although the activation energy reported for this stage, 70-110 kcal mol⁻¹, was lower than the present value, it seems likely that the same phenomenon occurred in the present experiments. It should be noted that the rapid reaction occurred above 160 °C in both techniques.

A final possibility may be mentioned as a cause of this rapid reaction. The presence of oxygen in the bomb may contribute to rapid secondary reactions during the decomposition. At the same time the large heat releases in any oxidation process could be an important factor in causing an increase in rate during the course of the reaction. Further experiments are planned to test this possibility

CLAIMS TO ORIGINAL RESEARCH

1. Kinetic data for the decomposition of Tetryl, including the temperature and pressure as a function of time, were determined using the ARC. Two stages in the decomposition were clearly distinguished.
2. Three methods for the derivation of the activation energy for decomposition from the data were used and evaluated. From data obtained using the Hastelloy C bomb, an activation energy of $52 \pm 1 \text{ kcal mol}^{-1}$ was obtained for the first stage and $43 \pm 1 \text{ kcal mol}^{-1}$ for the second stage.
3. The activation energies derived from the present data were compared with those obtained by other techniques. It was shown that measurements of the rate of decomposition under increasing temperature may give high values for the activation energy and the frequency factor.
4. The condensed-phase products of the decomposition of tetryl were analyzed at various stages of the decomposition. It was concluded that picric acid did not cause autocatalysis.
5. Data for the thermal decomposition of nitroguanidine in the solid state were obtained using the ARC.
6. Derivation of the activation energy for decomposition showed the large discrepancy in values obtained using data from the complete course of the reaction and using data from the initial stages only. These results showed the importance of autocatalytic process in the decomposition.

REFERENCES

1. S. Fordham; High Explosives and Propellants, Pergamon Press (1980).
2. Office Consolidation, Explosives Act and Explosives Regulations, Canada, August (1980).
3. J. Hák; Thermochemica Acta, 38, 253 (1980).
4. G.W. Taylor and G.H. Andrews, Jr.; Symposium on Chemical Problems Connected with the Stability of Explosives, pp 297 (1979).
5. D.I. Townsend and J.C. Tou; Thermochemica Acta 37, 1 (1980).
6. D.L. Chapman; Phil. Mag.[5], 47, 90 (1899).
- 7a. N.N. Semenov; Some Problems in Chemical Kinetics and Reactivity, vol. 2, (English translation by M. Boudart) Princeton University press (1959).
- 7b. D.A. Frank-Kamenetskii; Diffusion and Heat Transfer in Chemical Kinetics, (English translation by J.P. Appleton) Plenum Press, New York-London (1969).
8. P.H. Thomas; Trans Faraday Soc. 54, 60 (1958).
9. I. Verhoeff; Experimental Study of the Thermal Explosion of Liquids, Prins Maurits Laboratorium TNO, 1983.
10. P.P. Lee and R.R. Vandebek; Division report, MRP/MRL 83-35 (TR), Energy, Mines and Resources Canada.
11. P.P. Lee and R.R. Vandebek; Division report, ACEA/MRL 85-46 (CF), Energy, Mines and Resources Canada.
12. J.C. Tou and L.F. Whiting; Thermochemica Acta 48, 21 (1981).

13. L.F. Whiting and J.C. Tou; *J. of Thermal Analysis* 24, 111 (1982).
14. M.W. Duch, K. Marcali, M.D. Gordon, C.J. Hensler and G.J. O'Brien; *AICHE Plant/Operation Progress*, January (1982).
15. J.M. Pickard; *J. of Hazardous Materials* 7, 291 (1983).
16. T. Urbanski; *Chemistry and Technology of Explosives*, vol.3, Pergamon Press (1967).
17. C.D. Hutchinson; *Eighth International Symposium on Detonation*, pp 480 (1985).
18. R.C. Farmer; *J. Chem. Soc.* 117, 1603 (1920).
19. C.N. Hinshelwood; *J. Chem. Soc.* 119, 721 (1921).
20. A.J.B. Robertson; *Trans. Faraday Soc.* 44, 677 (1948).
21. M.A. Cook and M. Taylor Abegg; *Ind. Eng. Chem.* 48, 1090 (1956).
22. F.I. Dubovitskii, V.A. Strunin, G.B. Manelis and A.G. Merzhanov; *Russ. J. Phys. Chem.* 35, 148 (1961).
23. F.I. Dubovitskii, G.B. Manelis and L.P. Smirnow; *Russ. J. Phys. Chem.* 35, 255 (1961).
24. G. Krien; *Explosivstoffe* 13, 205 (1965a).
25. R.N. Rogers and E.D. Morris, *J. Anal. Chem.* 38, 413 (1966).
26. P.G. Hall; *Trans. Faraday Soc.* 67, 556 (1971).
27. Y. Hara, S. Kamei and H. Osada; *Kogyo Kagaku* 34, 253 (1973).
28. Y. Hara and H. Osada; *Kogyo Kagaku* 42, 298 (1981).
English Translation

29. C.E.H. Bawn; Chemistry of the Solid State, (Ed.) W.E. Garner, Butterworths, London (1955).
30. S.K. Yasuda; J. Chromatog. 50, 453 (1970).
31. J.B. Ainscough and E.F. Caldin; J. of the Chem Soc. 2528 (1956).
32. R. Foster; Nature 183,1042 (1959).
33. (Ed.) J.P. Phillips and F.C. Nachod; Organic Electronic Spectral Data, vol.1V, Interscience Publishers (1958).
34. Y. Hara, H.EDA and H. Osada; Kogyo Kagaku 36, 66 (1975).
35. S.M. Kaye; Encyclopedia of Explosives and Related Items, vol. 8, U.S. Army Armament Research and Development Command, Dover, New Jersey. p. p290 (1978).
36. E. Ripper and G. Krien; Explosivstoffe 17, 145 (1969).
37. Anon; Engineering Design Handbook, Headquarters, U.S. Army Material Command Pamphlet, AMCP 706-177, p.239 (1971).
38. J. Stals and M.G. Pitt; Aust. J. Chem. 28, 2629 (1975).
39. Y.P. Carignan and D.R. Satriana; The J. of Organic Chemistry 32, 285 (1967).
40. M.I. Eauth; Anal. Chem. 32, 655 (1960).
41. R.N. Rogers; Thermochemica Acta 11, 131 (1975).
42. R.N. Rogers; Thermochemica Acta 3, 437 (1972).
43. F. Volk; Ninth International Pyrotechnics Seminar, p.665 (1984).
44. V.V. Boldyrev; Thermochemica Acta 100, 315 (1986).